

**SYN-CONVERGENCE EXHUMATION OF CONTINENTAL CRUST:
EVIDENCE FROM STRUCTURAL AND METAMORPHIC
ANALYSIS OF THE MONTE CECU AREA, ALPINE CORSICA
(NORTHERN CORSICA, FRANCE)**

Journal:	<i>Geological Journal</i>
Manuscript ID	GJ-16-0058.R1
Wiley - Manuscript type:	Research Article
Date Submitted by the Author:	n/a
Complete List of Authors:	Di Rosa, Maria; University of Pisa, Scienze della Terra De Giorgi, Alberto; University of Pisa, Scienze della Terra Marroni, Michele; University of Pisa, Scienze della Terra; CNR, Istituto di geoscienze e Georisorse Vidal, Olivier; Université Grenoble, STerre,
Keywords:	deformation, high-pressure metamorphism, continental subduction, Piedigriaggio-Prato Unit, Alpine Corsica

SCHOLARONE™
Manuscripts

**SYN-CONVERGENCE EXHUMATION OF CONTINENTAL CRUST: EVIDENCE FROM
STRUCTURAL AND METAMORPHIC ANALYSIS OF THE MONTE CECU AREA,
ALPINE CORSICA (NORTHERN CORSICA, FRANCE)**

Di Rosa Maria¹, De Giorgi Alberto¹, Marroni Michele^{1,2,*}, Vidal Olivier³

¹ Dipartimento di Scienze della Terra, Università di Pisa, Italy.

² Istituto di Geoscienze e Georisorse, CNR, Pisa, Italy.

³ ISTerre, CNRS, Grenoble, France.

Running title: **Exhumation of continental crust in Alpine Corsica**

=====

* CORRESPONDING AUTHOR:
PROF. MICHELE MARRONI,
DIPARTIMENTO DI SCIENZE DELLA TERRA,
UNIVERSITÀ DI PISA, VIA S. MARIA, 53
56126 PISA, ITALY.
E-MAIL: marroni@dst.unipi.it

ABSTRACT

In the Corsica island, a stack of metamorphic continental units derived from the European continental margin is thrust over a pre-Alpine basement during the convergence-related processes in the Late Eocene-Early Miocene time span. The Piedigriggio-Prato Unit is representative of these units. Its tectono-metamorphic history has been reconstructed by an integrated approach, ranging from map- to meso- and microscopic scale analyses. This unit is characterized by a polyphase deformation history that consists of three deformation phases developed under retrograde metamorphism ranging from blueschist to sub-greenschist facies metamorphic conditions. At the map-scale, the Piedigriggio-Prato Unit is characterized by km-size isoclinal folds deformed by open to close recumbent folds producing Type 3 fold interference pattern. The features of the deformations and the P-T conditions suggest that the first two phases were acquired during the ductile extrusion of the Piedigriggio-Prato Unit. Before the Early Miocene, the gravitational collapse of over-thickened continental crust produced vertical shortening and the consequently recumbent F3 folds. The exhumation history of the Piedigriggio-Prato Unit can be view as representative for the exhumation of a continental crust fragment during the transition from the continental subduction to the continental collision.

Keywords: high-pressure metamorphism, continental subduction, exhumation, Piedigriggio-Prato Unit, Alpine Corsica.

1. INTRODUCTION

The Corsica Island is regarded as a lithospheric boudin located between two back-arc basins of Neogene-Quaternary age (e.g. Gueguen *et al.*, 1998). This boudin preserves fragments of the alpine belt, i.e. Alpine Corsica, that consists of a stack of oceanic and continental units issued from the Ligure-Piemontese oceanic basin and the European continental margin, respectively (e.g. Boccaletti *et al.*, 1971; Durand-Delga, 1984, Malavieille *et al.*, 1998). These units recorded a polyphase tectono-metamorphic history acquired in the Late Cretaceous-Early Tertiary time span during the closure of the Ligure-Piemontese oceanic basin and the subsequent continental collision. In this framework, a stack of continental units affected by high-pressure (HP) metamorphism during the Early Tertiary has been recognized in the last thirty years in the western areas of Alpine Corsica (e.g. Gibbons and Horak 1984; Daniel *et al.*, 1996; Tribuzio and Giacomini, 2002; Garfagnoli *et al.*, 2009, Maggi *et al.*, 2012; Rossetti *et al.*, 2015 and references therein). These continental units were deformed when the European continental margin, still attached to the downgoing oceanic slab, was subjected to underthrusting, accretion and subsequent exhumation. Since the plate convergent rate and the geothermal gradient change during the plate subduction, the style of deformation, the metamorphic conditions as well as the mechanisms that produce exhumation of HP continental rocks change with time (Cloos, 1982; Platt, 1986; Dewey *et al.*, 1993; Steck *et al.*, 1998; Chemenda *et al.*, 1995; Thompson *et al.*, 1997; Guillot *et al.*, 2001; Jolivet *et al.*, 2003).

To study in detail the tectono-metamorphic history of a fragment of the European continental margin during the continental subduction, we conducted meso- to micro-scale structural and thermo-baric investigations in one of these continental units, known as the Piedigriggio-Prato Unit (Malasoma *et al.*, 2006). The unit is well-exposed north of Corte in the Monte Cecu area (Fig. 1) and any information about its structural and metamorphic history is lacking. The results of this study give the opportunity to elaborate a P-T-d (pressure-temperature-deformation) path and to discuss the processes that produced the exhumation of continental units during the convergence-related processes. The results of this study are also discussed in the framework of the Alpine Corsica tectonic evolution.

2. GEOLOGICAL FRAMEWORK

From the geological point of view, the Corsica Island is divided into two domains, known as Hercynian and Alpine Corsica (e.g. Durand-Delga, 1984), which crop out in the south-west and north-east areas, respectively (Fig. 1). The tectonic boundary between these two domains runs across the island with a NNW-SSE strike along which the tectonic units of Alpine Corsica are thrust

97 onto Hercynian Corsica (e.g. Durand-Delga, 1984). However, this tectonic boundary is partially
 98 reworked by the Central Corsica Shear Zone (CCSZ in Fig. 1), a strike-slip system originated in the
 99 Late Eocene-Early Oligocene time span (Lacombe and Jolivet, 2005).

100 Hercynian Corsica is representative of a continental crust of the European plate. It consists of
 101 metamorphic rocks with Panafrican and Variscan metamorphic and deformation imprints that are
 102 intruded by magmatic rocks of Permo-Carboniferous age (Cabanis *et al.*, 1990; Ménot, 1990;
 103 Laporte *et al.*, 1991; Paquette *et al.*, 2003; Rossi *et al.*, 2009). This basement is covered by
 104 sedimentary successions consisting of Mesozoic deposits, mainly carbonates. Along the tectonic
 105 boundary between Hercynian and Alpine Corsica, siliciclastic turbidites of Tertiary age lay in
 106 angular unconformity on both the basement and the Mesozoic deposits (Durand-Delga, 1984, Rossi
 107 *et al.*, 1994; Michard and Martinotti, 2002).

108 Alpine Corsica and Western Alps were separated since the Early Oligocene time by the
 109 Ligure-Provençal Basin (e.g. Gueguen *et al.*, 1998) opened between the European and Adria plate
 110 continental margins consequently to the the Jurassic spreading phase (e.g. Marroni and Pandolfi,
 111 2007). Similarly to the Western Alps, the structural setting of Alpine Corsica derived from the
 112 closure of the Ligure-Piemontese oceanic Basin and the subsequent deformations of the paired
 113 continental margins during the Late Cretaceous-Tertiary time span (Malavieille *et al.*, 1998; Molli
 114 and Tribuzio, 2004; Marroni *et al.*, 2010). The convergence between European and Adria plates (the
 115 onset of which is still matter of debate, see discussion in Vitale Brovarone and Herwartz, 2013)
 116 started with an intraoceanic subduction leading to the development of an accretionary wedge made
 117 by imbricated oceanic units overprinted by HP metamorphism (Mattauer *et al.*, 1977; Caron and
 118 Delcey, 1979; Faure and Malavieille, 1981; Harris, 1985; Warburton, 1986; Waters, 1990; Fournier
 119 *et al.*, 1991; Malavieille *et al.*, 1998; Levi *et al.*, 2007; Chopin *et al.* 2008; Ravna *et al.* 2010; Vitale
 120 Brovarone and Herwartz, 2013). The intraoceanic subduction was followed by the continental
 121 subduction, whose inception was marked by the involvement of thinned continental margin in the
 122 subduction zone, probably during Early Tertiary time (e.g. Mattauer and Proust, 1976; Mattauer *et*
 123 *al.*, 1981; Gibbons and Horak 1984; Bezert and Caby 1988; Egal, 1992; Daniel *et al.*, 1996; Brunet
 124 *et al.*, 2000; Tribuzio and Giacomini, 2002; Malasoma *et al.*, 2006; Molli *et al.*, 2006; Marroni *et*
 125 *al.*, 2010; Molli and Malavieille, 2011; Maggi *et al.*, 2012). During the subsequent continental
 126 collision, an orogenic belt made up of a continental and oceanic units was formed. Since Early
 127 Oligocene time, the compressional tectonics in Corsica was followed by large-scale extension
 128 leading to the collapse of the previously thickened orogenic wedge (Fournier *et al.*, 1991; Jolivet *et*
 129 *al.*, 1991; Daniel *et al.*, 1996; Brunet *et al.*, 2000; Zarki-Jakni *et al.*, 2004). During Early Miocene
 130 time, the opening of the Liguro-Provençal and the Thyrrenian Basins isolated the Sardinia-Corsica

microplate and consequently, the Alpine Corsica from the neighbouring domains of the Alpine collisional belt (Doglioni *et al.*, 1998; Mauffret *et al.*, 1999; Fellin *et al.*, 2005).

The processes of subduction and subsequent continental collision can be fully documented investigating the deformation and the associated metamorphism recorded by the tectonic units stacked in the Alpine Corsica. These units are generally divided in three groups according to their stratigraphical and structural features (e.g. Durand-Delga, 1984; Jolivet *et al.*, 1990; Malavieille *et al.*, 1998; Marroni and Pandolfi, 2003; Molli, 2008). From the bottom to the top, they are: the Lower Units (also known as Corte Units or Parautochthonous or Prépiémontais), the Schistes Lustrés complex and the Upper Units (also known as Nappe Supérieure).

The Lower Units are interpreted as fragments of the thinned European continental margin accreted to the Alpine orogenic wedge in the Tertiary time. These continental-derived tectonic units (i.e. Centuri Unit, Serra di Pigno Unit, Caporalino Unit, Corte Units, Annunciata Unit and Tenda massif) mainly consist of slices of Variscan basement and its Late Carboniferous-Middle Eocene sedimentary cover. Generally, they are characterized by a polyphase deformation and by Alpine-age metamorphism ranging from very low-grade to blueschist facies conditions (Bezert and Caby 1988; Molli *et al.*, 2006; Malasoma and Marroni, 2007; Molli, 2008).

The Schistes Lustrés are a group of tectonic units of both oceanic and continental affinity, which were intensely deformed during their subduction and accretion to the orogenic wedge. The HP peak metamorphic conditions documented in the Schistes Lustrés ranged from blueschist to eclogite facies while the retrogressive metamorphism developed under blueschist and greenschist facies conditions (Gibbons *et al.*, 1986; Warburton, 1986; Waters, 1990; Fournier *et al.*, 1991; Caron, 1994; Daniel *et al.*, 1996; Vitale Brovarone *et al.*, 2011). According to the available data, the age of the HP-LT metamorphism ranges from Late Cretaceous to Early Oligocene (Maluski, 1977; Lahondère and Guerrot, 1997; Brunet *et al.*, 2000; Maggi *et al.*, 2012; Martin *et al.*, 2011; Vitale Brovarone and Herwatz, 2013; Rossetti *et al.*, 2015).

The Upper Units (i.e. Balagne Unit, Nebbio Unit, Macinaggio Unit, Bas Ostriconi Unit, Rio Magno Unit, Pineto Unit, and Santa Lucia Unit) consists of continental and oceanic units affected by a very low-grade metamorphism. They are mainly represented by ophiolitic units (Balagne and Nebbio Units) consisting of a Jurassic ophiolite sequence and related Late Jurassic-Late Cretaceous sedimentary cover (Durand Delga, 1984; Durand-Delga *et al.*, 1997; Saccani *et al.*, 2000; Padoa *et al.*, 2001; Rossi *et al.*, 2002; Marroni and Pandolfi, 2003). The Balagne and Nebbio Units are generally associated with the Macinaggio and Bas-Ostriconi Units, consisting in turn of Late Cretaceous carbonate turbidites (Sagri *et al.*, 1982; Dallon and Nardi, 1984; Durand-Delga, 1984; Pandolfi *et al.*, 2016).

The relationships between Lower Units, Schistes Lustrés and the Upper Units are sealed by the Early Miocene deposits of the Saint Florent and Francardo basins (Dallan and Puccinelli, 1995; Ferrandini *et al.*, 1998; Cavazza *et al.*, 2001), both opened during the post-collisional extensional regime that affected Alpine Corsica.

3. TECTONIC SETTING OF THE CORTE AREA

The study area is located in the centre of the Corsica Island, between Castirla, Francardo and Corte (Figs. 1 and 2). The Corte area is characterized by a stack of three continental units belonging to the Corte Units (i.e. Lower Units) sandwiched between the Hercynian Corsica in the west, and the Schistes Lustrés in the east (Fig. 1b).

Hercynian Corsica, here represented by Permo-Carboniferous granitoids and their metamorphic host rocks, is unconformably covered by Middle to Late Eocene unmetamorphosed siliciclastic turbidites. Even if it is classically considered as an autochthonous domain escaped by the Alpine tectonics (Amaudric du Chaffaut, 1975; Durand-Delga, 1984; Rossi *et al.*, 1994), the occurrence of shear zones west of the study area suggests that it was affected by a post-Variscan deformations.

The continental units cropping out in the study area are bounded by east-dipping shear zones. From west to east, they are (Figs. 1 and 2): the Castiglione-Popolasca Unit, the Croce d'Arbitro Unit and the Piedigriggio-Prato Unit. They show a similar lithostratigraphy and recorded the same HP metamorphic imprint. Malasoma and Marroni (2007) reported $P = 6 \pm 1.5$ kbar and $T = 325 \pm 20$ °C for the metamorphic peak in the Castiglione-Popolasca Unit, whereas Malasoma *et al.* (2006) reported $P = 5\text{--}8$ kbar and $T = 300\text{--}370$ °C in the Croce d'Arbitro Unit. No pressure and temperature estimates are available in literature for the metamorphic peak recorded in the Piedigriggio-Prato Unit.

In the Corte area, the Schistes Lustrés, usually occurs at the top of the stack of continental units. However, slices of this complex have been also recognized along the boundaries between the different continental units.

4. THE PIEDIGRIGGIO-PRATO UNIT

The Piedigriggio-Prato Unit occurs at the top of the stack of the continental units cropping out in the Corte area. Although the evidence of tectonic delaminations, the good outcrops exposure (especially in the Monte Cecu area) and the detailed fieldwork conducted in the area allow to reconstruct the stratigraphy of this unit. The complete stratigraphic log is shown in Fig. 3. Our

reconstruction is in good agreement with the picture previously proposed by Amaudric du Chaffaut (1975) and Rossi *et al.* (1994).

4.1. Stratigraphic log

The stratigraphic log of the Piedigriggio-Prato Unit includes a basement consisting of poly-metamorphic rocks (i.e. Roches Brunes Fm., **RB**) of Panafrican age (Rossi *et al.*, 1994) intruded by Permo-Carboniferous metagranitoids (**Mg**) (Ménot, 1990; Laporte *et al.*, 1991; Paquette *et al.*, 2003) and covered by Permo-Carboniferous metavolcanites and metavolcanoclastites (**Mv**). The basement is unconformably covered by metamorphic rocks whose protoliths are represented by sedimentary rocks (mainly carbonate) of **Mesozoic** age. The upper portion of the stratigraphic log is represented by a thick succession of siliciclastic metabreccias and metarenites deposited in discordance on the Mesozoic rocks probably during the **Middle-Late Eocene**. On the whole, this stratigraphic log testifies the Mesozoic-Early Tertiary evolution of the thinned European continental margin (Dallan and Nardi, 1984; Durand-Delga, 1984, Rossi *et al.*, 1994).

In the study area, the basement of the Piedigriggio-Prato Unit is missing and the succession starts with the Mesozoic carbonate of the Metadolomies Fm. (**Md**) cropping out northwest of Bistuglio village. The Metadolomies Fm. (Norian: Rossi *et al.*, 1994) is characterized by thick layers of metadolomies alternating with purple metapelites, interpreted as paleosoils horizons. The Metadolomies Fm. shows a transition to the Metaconglomerates Fm. (**Mc**) (Fig. 3) that is recognized as discontinuous lenses consisting of fragments of metadolomies and metavolcanites in a carbonate matrix. Ritsema (1952) interpreted the fragments of metavolcanites as evidences of a volcanic episode of Norian age. The Metadolomies and Metaconglomerates Fms. are both topped by the Metalimestones and Metadolomies Fm. (**MM**) consisting of medium thick beds of metalimestones and metadolomies (Fig. 3). The age of this formation is Hettangian - Sinemurian based on correlation with Monte Tuda limestones (Nebbio Unit) containing fossils of *Gryphea Cf. Arcuata* (Rossi *et al.*, 1994). The succession continues with the Hettangian - Sinemurian Lumachella Metalimestones Fm. (**LM**) showing a well-preserved association of *lamellibranchs, bryozoa and echinids*. The Lumachella Metalimestones Fm. is not continuous across the whole study area, but when recognized, it shows a transition to the Thin-bedded Metalimestones Fm. (**TM**) of Liassic age (Rossi *et al.*, 1994) represented by thin beds of metalimestones alternating with very thin beds of metapelites. At the top of the Thin-bedded Metalimestones Fm., discontinuous lenses of Cherty Metalimestones Fm. (**CM**) occur. The last formation of Mesozoic age is represented by the Detritic Metalimestones Fm. (**DM**) of Liassic age consisting of a matrix-supported polymict metabreccias, often characterized by well-graded beds. The Mesozoic succession is unconformably

topped by the Metabreccias Fm. (Mb) showing a stratigraphic, gradual upward transition to the Metaturbidites Fm (Mt).

The Metabreccias Fm. consists of subrounded to subangular clasts of orthogneisses, paragneisses, micaschists, metagranites, quartzites and marbles wrapped by a fine-grain matrix ranging in size from metapelites to metarenites. At the top of Metabreccias Fm., the Metaturbidites Fm. (Mt) crops out as medium beds of metarenites and metapelites. The intervals of Bouma sequence are still well recognizable. The occurrence of *Nummulites sp.* indicates a Middle to Late Eocene age for the Metaturbidites Fm. (Rossi *et al.*, 1994). For the Metabreccias Fm., Amaudric du Chaffaut (1975) suggested a Late Cretaceous age, based on the presence of metacarbonatic clasts. Rossi *et al.* (1994) correlated the Metabreccias Fm. of Corte area with those of Caporalino area, that are assigned to a Dogger age. However, the clear gradual stratigraphic transition between Metabreccias and Metaturbidites Fms. suggests the same age for these formations. Thus, a Middle to Late Eocene age for the Metabreccias Fm. is proposed in this paper.

4.2. Micro- and meso-scale deformation history

The Piedigriggio-Prato Unit is characterized by a complex tectonic setting derived from the overprinting of three phases of ductile deformations (D1, D2 and D3) that can be recognized at all the scales of observation (Fig. 4). The three deformation phases produced pervasive folding and foliation. The D1 phase are almost completely disrupted by later D2 deformation, which produced the most widespread structures in the field and the most important map-scale structures. The last D3 deformation phase refolds all the pre-existing tectonic structures.

In the eastern portion of the study area, the structures related to D1, D2 and D3 phases are cut by a system of brittle strike-slip faults belonging to the Central Corsica Fault Zone. These brittle deformations are not discussed in this paper.

4.2.1 D1 phase

Rare relics of the D1 phase can be identified in the field. They are represented by folded quartz veins, by very rare isoclinal sheath folds (documented only in the Detritic Metalimestone Fm. at the top of Monte Cecu) and by rare relics of S1 foliation preserved within the hinges of the F2 folds, in the Metaturbidites Fm. (Fig. 4a). The S1 foliation shows NNE-SSW strike and vertical dip (Fig. 5).

At the microscale, the relics of the D1 phase were recognized within D2 microlithons preserved within mm-thick metapelites layers (e.g. within the Metabreccias and the Metaturbidites Fms). These relics are represented by a transposed S1 foliation (Fig. 4e) that occurs as a well-developed and continuous anisotropy defined as a schistosity. Locally, the S1 foliation wraps quartz

and feldspar porphyroclasts. In metapelites, relics of the minerals assemblage grown during the D1 phase are represented by quartz, white mica and chlorite. In the metalimestones, large boudinated crystals of calcite show Type 2 mechanical twins (Burkhard, 1993) probably acquired during the D1 phase (Fig. 4d).

4.1.2 D2 phase

The structures related to the D2 phase represent the main structures documented in the field. In the metalimestones, metapelites, metarenites and metabreccias, the S2 foliation is a pervasive and continuous anisotropy. In the Metabreccias Fm., it is associated with a flattening of the clasts that reached a R_{xz} ratio of 10:1 (Fig. 4b). In the study area, the S2 foliation shows a NNE-SSW strike with a dipping ranging from horizontal to vertical as results of the overprinting of the D3 phase (Fig. 2). On the S2 foliation, the mineral lineation L2 is represented by elongated chlorite, quartz and white mica whereas the L2 stretching lineations, mainly observed in the metalimestones, are represented by boudinated millimetre-sized pyrite and quartz grains with oriented growth of calcite fibres. Both mineral and stretching lineations display a preferred orientation showing a dominant ESE-WNW trend. The other most widespread structure produced during the D2 phase is represented by the sub-isoclinal to isoclinal F2 folds, showing limbs often affected by necking and boudinage. The A2 axes trend roughly N-S with shallow plunge (Fig. 5). At the boundaries and inside the Piedigrioglio-Prato Unit, the D2 phase produced also shear zones marked by cataclasites with well-developed S-C structures.

At the microscopic scale, the S2 foliation documented along the limbs of the F2 folds in metapelites and metarenites is a continuous and pervasive foliation highlighted by the growth of new metamorphic minerals (Fig. 4c). In these domains, the main foliation is represented by a composite layering defined by the overprinting of S2 foliation on the S1 one. In contrast, in the F2 hinge-zone, where the S1 foliation is still preserved, the S2 foliation can be classified as crenulation cleavage, characterized by smooth cleavage domains showing a gradational to discrete transition to the microlithons. The S2 foliation is characterized by syn-kinematic recrystallization of white mica, quartz, calcite, chlorite and albite. Within the shear zones located at the boundaries and inside the Piedigrioglio-Prato Unit, the kinematic indicators, represented mainly by σ -type porphyroclasts of quartz and synthetic and antithetic microfaults in large porphyroclasts suggest a top-to-W sense of shear. The metalimestones are recrystallized during the D2 phase with development of a fine-grained granoblastic texture. Recrystallized crystals of calcite show twins belonging to Type 2 of Burkhard (1993) classification.

4.1.3 D3 phase

D3 phase, mainly represented by open F3 folds with rounded hinges and sub-horizontal axial planes (Fig. 2), deform everywhere the structures related to D1 and D2 phase. The interlimb angle of F3 folds range from 90° 140°. The A3 axes show a NNE-SSW trend and sub-horizontal plunge. The interference pattern between D2 and D3 phases, visible at all the observation scales and in all the formations, can be referred to type 3 (Ramsay, 1967).

At the outcrop scale, the S3 foliation occurs as a convergent fanning axial-plane crenulation cleavage in the metapelites and metarenites whereas in the metalimestones it is represented by a disjunctive cleavage. At the microscale, the S3 foliation in metapelites is classifiable as crenulation cleavage where the main deformation mechanism is represented by pressure solution and reorientation of pre-existing tabular grains (Fig. 4f). Minor recrystallization of quartz, calcite and Fe-oxides also occurs. Type 1 calcite twins (Burkhard, 1993) indicate deformation temperature of <200°C.

4.3. Map scale structures

The study area is characterized by well-developed map-scale structures (Fig. 2) that can be related to the D2 and D3 phases. No map-scale structures are related to D1 phase. The structures related to the D2 phase are represented by F2 isoclinal antiforms and synforms with well-developed reverse limbs dipping about 40° to the east. The most important F2 fold is the antiform located in the southern slope of Monte Cecu (Figs. 1 and 2). Its normal and overturned limbs dip toward east and the core is represented by the Metadolomies Fm. (Fig. 2). Related to this structure, two synforms with the Metaturbidites Fm. at the core have been identified in the western slopes of Monte Cecu (Fig. 2). In the hinge zones of these synforms, the interference between S1 and S2 foliations can be observed also at mesoscale. The F2 folds show A2 axes trending N-S with gently plunges northward and AP2 axial planes striking N-S. The AP2 show a variable dip, from sub-vertical to sub-horizontal, as the consequence of the F3 folds overprinting.

The D3 phase produces open to close F3 folds, characterized by westward shallow dipping axial plane (Fig. 2). The F3 folds also deform the shear zones highlighting the tectonic contacts between the continental units and the slices of Schistes (see the geological cross-section in Fig. 2).

4.4. Metamorphic P-T conditions

To characterize the metamorphic conditions of the Piedigriggio-Prato Unit, about 10 samples were collected in the Monte Cecu area within the Metabreccias Fm.. Among them, two samples (CM21 and CM32C) were selected for the analyses. In these samples, the S1 and S2 foliations are

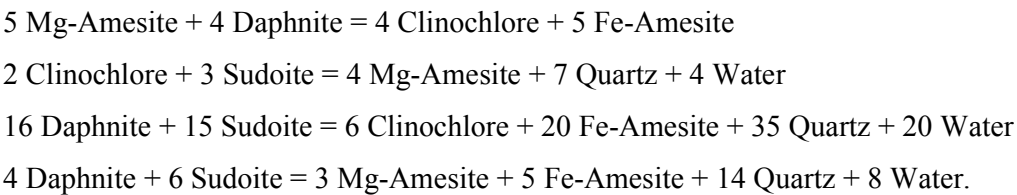
characterized by a different chlorite + white mica metamorphic assemblages, all showing a size suitable for microprobe analysis. The occurrence of specific mineral assemblages in both foliations was regarded as the result of different P-T equilibrium conditions reached during the D1 and D2 phases.

The electron probe data have been acquired with a JEOL JXA – Electron probe microanalyzer (EPMA) equipped with five wavelength-dispersive spectrometers and treated with XMapTools, a MATLAB based graphic software for processing of X-ray images (Lanari *et al.*, 2014). XMapTools requires data acquired under 15 KeV accelerating voltage, 10-100 nA specimen current and a 300 ms per grid point counting time. For each mineral, a series of pixels were measured under standard conditions (pure Al₂O₃ (Al), wollastonite (Ca), pure Fe₂O₃ (Fe), orthoclase (K), diopside (Mg, Si), rhodonite (Mn), albite (Na), apatite (P), pure TiO₂(Ti)) and the results were used as internal standard to transform maps of photon intensity into maps of elements concentration (De Andrade *et al.*, 2006; Lanari *et al.*, 2014). Maps of structural formulae and compositional diagrams were computed with XMapTools, and thermodynamic calculations were conducted with an unpublished MATLAB based graphic software using the thermodynamic data and solid solution models of Vidal *et al.* (2006) for chlorite and Dubacq *et al.* (2010) for K-white mica.

4.4.1 Chlorite-Quartz-Water geothermometer

The structural formulae of chlorites were calculated assuming 14 anhydrous oxygens. The chlorite compositions from CM21 and CM32C samples calculated with $Fe^{tot} = Fe^{2+}$ are plotted in a Si/XMg diagram and show Si contents from 3.45 to 4.4 apfu, while the XMg from 0.43 to 0.68 apfu, with higher values for CM21 sample (Fig. 6a).

The formation temperature and Fe^{3+} content of chlorite in Metabreccias Fm. was estimated at P = 5 kbar according to the approach proposed by Vidal *et al.* (2006) which is based on the convergence of the following equilibria, assuming unit activity of water:



Temperatures and Fe^{3+} contents were calculated by successive iterations of the Fe^{3+} amount until convergence of equilibria 1 to 4 to within 50°C. Chlorite in CM21 and CM32C samples was found to crystallize at temperature ranging from 252 to 357°C, with an average value of $304 \pm 50^\circ\text{C}$ (Tab. 1, Fig. 7).

4.4.2 Phengite-Quartz-Water *geobarometer*

The structural formulae of white micas were calculated assuming 11 anhydrous oxygens. The compositions of phengites, intergrown with chlorite in S1 and S2 foliations, show Si contents between 3.6 and 3.3 apfu (Fig. 6b); an enrichment in Al^{IV} and a depletion in Si content of the CM21 sample compared to the CM32C is observed.

The estimation of pressure based on phengite composition is a technique proposed by many authors (Velde, 1965; Massonne, 1998; Massonne and Szpurka, 1997; Parra *et al.*, 2002). This approach is generally based on the Si-content of phengite that occurs in a given buffering mineral assemblage, such as k-feldspar, phlogopite, quartz and water (Massonne and Schreyer, 1987; Massonne and Szpurka, 1997). In our samples, biotite is replaced by chlorite, which suggests a possible lack of equilibrium with phengite during the latest stage of the metamorphic history. It follows that only minimum pressure conditions ranging from 8.3 to 10.4 kbar could be estimated for the phengites of sample CM21 and sample CM32C (Tab. 2); these phengites are in equilibrium with the chlorites on which the geothermometer, previously applied, provided an average temperature of 304°C.

4.4.3 The Chlorite-Phengite-Quartz-Water multi-equilibrium approach

The coexistence of several chlorite and phengite generations, grew in different microstructural sites and showing different compositions, was used to constrain the P-T evolution of Metabreccias Fm. with an approach similar to that used proposed by Parra *et al.* (2002), Vidal *et al.* (2006) and Lanari *et al.* (2012).

Chlorite-phengite pairs that grew in the same microstructural site were selected from maps of minerals composition acquired and treated with XMapTools. The P-T conditions of chlorite-mica equilibrium (Fig. 8) were calculated using the solid solution model of Parra *et al.* (2002) for phengite completed with the H₂O-K-Na-vacancy interactions in the interlayer position as modelled by Dubacq *et al.* (2010). This method has two main sources of errors (Vidal and Parra, 2000): 1) uncertainties associated with the thermodynamic data and solid solution models, which are difficult to estimate because the thermodynamic standard state properties are calibrated using experimental and natural data of various levels of confidence, and 2) analytical errors associated with the measure of compositions and their standardization (De Andrade *et al.*, 2006). To account for these errors, a certain degree of P-T estimates scatter between the calculated equilibria is accepted, although in theory, all equilibria should intersect at a single P-T point. In the elemental map realized for the selected sites, the phengite-chlorite pairs were chosen manually to check if there are any relationship between the microstructures and the variations in compositions.

In sample CM21 the older generation of phengites grew along the S1 foliation and show a 50-65% muscovite end-member. The P-T conditions recorded at their equilibrium with the chlorite grown along the S1 foliation are $P = 6.2 - 7.5$ kbar and $T = 290-310^{\circ}\text{C}$. A second growth of phengite-chlorite pairs grew in equilibrium on the S1 foliation provided $P = 5.1 - 6$ kbar and $T = 350-400^{\circ}\text{C}$. The third generation of phengites grew along the S2 foliation in association with chlorites. The phengites have a lower content in muscovite end-member (40%) whereas chlorites show lower amesite contents respect to the chlorites in equilibrium at higher temperatures. The equilibrium conditions related to this third generation of phengite -chlorites pairs are $P = 2.3-3.8$ kbar and $T = 240-300^{\circ}\text{C}$ (Figs. 9 and 10). The same observations could be made for sample CM32C. The P-T equilibria conditions for the first generation of phengite-chlorite couples are $P = 6.7-10.4$ kbar and $T = 200-350^{\circ}\text{C}$, while the second generation provided P-T equilibria conditions of $P = 3.1 - 3.5$ kbar and $T = 250-280^{\circ}\text{C}$ (Tab. 3).

4.5 Deformation-metamorphism relationships

The metamorphic results obtained in the Metabreccias Fm. and the structural data collected at the micro- and mesoscopic scale provide valuable constraints for the relationships between deformation and metamorphism in the Piedigiglio-Prato Unit.

As described in the previous section, the P-T paths obtained from the selected samples are characterized by: (1) a baric peak (HP-LT event) at $P = 7.5-10.4$ kbar and $T = 200-240^{\circ}\text{C}$, (2) a thermic peak (LP-HT event) characterized by $P = 5.1-8$ kbar and $T = 340-400^{\circ}\text{C}$ and (3) a another field of stability (LP-LT event) at $P = 2.3-3.8$ kbar and $T = 240-300^{\circ}\text{C}$. Metamorphic and structural textural relationships indicate that both the HP-LT and the LP-HT events were documented exclusively by chlorite-phengite pairs grown parallel to the S1 foliation (i.e. preserved within D2 microlithons), while the LP-LT event was documented by chlorite-phengite pairs recrystallize along the S2 foliation (Fig. 10).

These data clearly indicate that the retrograde path of the Piedigiglio-Prato Unit started during the late stages of the D1 phase (Fig. 11). The exhumation path is characterized by a transition from high- (HP-LT event) to low- (LP-HT event) pressure conditions during an increase of temperature that allow the crystallization of high-temperature chlorite end-member. During the D2 phase, a new generation of chlorites and phengites (LP-LT event) grew along to the S2 foliation. P-T conditions, that are lower than those achieved during D1 phase, are coherent with a deformation at shallow structural level. On the whole, these complex polyphased deformation history, developed during a retrograde metamorphism is connected to the progressive exhumation of the Piedigiglio-Prato Unit.

4.6. Age constraints

Owing to the lack of radiometric datings, the ages of deformation affecting the continental units cropping out at the eastern border of Hercynian Corsica (i.e. Corte Units) is constrained considering: 1) the youngest age of the rocks involved in the deformation and 2) the age of the sediments that unconformably seal the stack of the tectonic units.

In the study area, the youngest formation is represented by the Metaturbidites Fm. According to the occurrence of *Nummulites sp.* (Rossi *et al.*, 1994), its depositional age is constrained at the Middle - Late Eocene. This age is coherent with that estimated using Bartonian foraminifera in the metarenites in the Castiglione-Popolasca Unit (Bezert and Caby, 1988) that indicates that the deformation and metamorphism in this unit is post 37.8 Ma (Gradstein *et al.*, 2012). This constraint can be extended to the other continental units of the Corte area. In addition, about 5 km north of the study area, the stack of the continental units is covered by a marine to continental sedimentary succession cropping out in the Francardo area (Ferrandini *et al.*, 2003). The base of this succession has been assigned to Burdigalian (20.4 Ma; Gradstein *et al.*, 2012) by Alessandri *et al.* (1977). Thus, the deformation and metamorphism related to underthrusting, accretion and exhumation history of the continental units seem to be developed in about 17 Ma time span from Late Eocene to Early Miocene.

5. DISCUSSION

The geodynamic scenario proposed for the Alpine belt (e.g. Handy *et al.*, 2010 and quoted references) at the end of the oceanic subduction requires the involvement of the thinned European margin into tectonic processes related to continental subduction and subsequent collision (e.g. Schmid *et al.*, 1996; Stampfli *et al.*, 1998; Handy *et al.*, 2010). During the continental subduction, the thinned continental crust of the European plate underwent to progressive deformation during underthrusting and subsequent exhumation into the orogenic wedge, as evidenced by the metamorphic continental units from the Western Alps (e.g. Oberhänsli *et al.*, 2004). In this scenario, the collected data about the lithostratigraphy and the structural and metamorphic evolution of the Piedigriggio-Prato Unit allow to reconstruct the tectono-metamorphic history of a continental fragment involved in the continental subduction and subsequent collision.

The lithostratigraphic setting of the Piedigriggio-Prato Unit clearly indicates its origin from the continental margin of the Europe plate. This continental margin experienced a sinking from Trias to Early Jurassic with a progressive deepening associated to extensional, rifting-related

1
2 480 faulting that controlled the sedimentation in the whole European margin (e.g. Durand-Delga, 1984).
3 481 No information about the Cretaceous history was preserved. However, the most important feature of
4 482 this succession is the unconformity that occurs at the base of the Middle to Late Eocene
5 483 Metabreccias and Metaturbidites Fms. In this time span, the continental crust was already involved
6 484 in the continental subduction processes whose inception is regarded as Paleocene in age (Maggi *et*
7 485 *al.*, 2012 and quoted references). In this setting, the European continental margin is affected by a
8 486 flexural bending producing an uplifted forebulge deformed by extensional tectonics with normal
9 487 faulting and block tilting (Sinclair, 1997; Ford *et al.*, 1999). The normal faults were probably
10 488 originated by reactivation of former Jurassic faults as the European continental crust was
11 489 approaching the foredeep basin. The extensional tectonics produced denudation of the Triassic to
12 490 Jurassic stratigraphic levels that were immediately covered by foredeep deposits supplied by the
13 491 European continental domain. An unconformity analogous to the Piedigrosso-Prato Unit was
14 492 recognized, for instance, in the Briançonnais domain in the Alps (e.g. Michard and Martinotti,
15 493 2002) and in oceanic domain in northern Apennines (e.g. the Internal Ligurian Units; Marroni and
16 494 Pandolfi, 2001).

17 495 The structural and metamorphic data collected in the Piedigrosso-Prato Unit provides
18 496 important information about its implication into the Alpine orogenic wedge. The oldest deformation
19 497 phase documented in the Piedigrosso-Prato Unit produced a S1 foliation. Thermodynamic
20 498 calculations conducted on recrystallized chlorite-phengite pairs grown along the S1 foliation
21 499 indicate that the D1 phase was developed between P = 7.5-5.1 kbar and T = 290-400°C in sample
22 500 CM21 and between P = 10.4-6.7 kbar and T = 200-350°C in the sample CM32C (Fig. 11). The P-T
23 501 conditions for D1 thus correspond to geothermal gradients between 6.3° and 25.9°C/Km. Such
24 502 values are coherent with those estimated for the continental crust involved in the subduction (e.g.
25 503 Ganne *et al.*, 2007) and with those estimated for the Briançonnais units in the Western Alps (e.g.
26 504 Lanari *et al.*, 2014 and quoted references). They are also in agreement with the geothermal
27 505 gradients obtained from the other continental units from Alpine Corsica (e.g. Malasoma and
28 506 Marroni, 2007, Vitale Brovarone *et al.*, 2013).

29 507 The most significant finding of this work is the report of a pressure decrease and a
30 508 simultaneous temperature increase during the growth of chlorite and phengite along the S1 foliation.
31 509 The P-T estimates are corroborated by the high content of Al and Fe - Mg of chlorites grew along
32 510 the S1 foliation that indicates an increase of the temperature, compared to the other chlorites that
33 511 occur in the S1 foliation, similar in Fe - Mg content but poorer in Al content. These Al-poor
34 512 chlorites are older than the Al-rich ones and are in equilibrium with the highest-pressure phengites
35 513 that grew on the S1 foliation. These data indicate that the S1 foliation developed under decreasing
36 514 pressure and increasing temperature conditions, suggesting that the D1 phase was acquired during

the exhumation of Piedigriggio-Prato Unit. The exhumation continues during the D2 phase that is characterized by sub-isoclinal to isoclinal F2 folds, the associated foliation and localized shear zones. The recrystallized pairs chlorite-phengite grew along the S2 foliation, provided P-T conditions of $P = 2.3\text{--}3.1$ kbar and $T = 240\text{--}300^\circ\text{C}$. The P-T conditions for D2 phase thus correspond to geothermal gradients between 26.4° and 34.4°C/Km , calculated between the LP-HT event (i.e. late D1 phase) and the LP-LT (i.e. D2 phase). On the whole, the D1 and D2 phase produced the continuous exhumation of the Piedigriggio-Prato Unit from an **estimated depth of about 31.5 km up to about 7 km**. The D2 shear zones, localized at the boundaries of the Piedigriggio-Prato Unit, were responsible of the top-to-the-west thrusting of the unit onto the other continental units that are in turn thrust **over** Hercynian Corsica and its sedimentary cover (e.g. Molli and Malavieille, 2011).

Based on these observations, the exhumation of the Piedigriggio-Prato Unit during the D1 and D2 phases occurred by ductile extrusion (**Fig. 12**). The same exhumation history may be suggested for the other continental units of Alpine Corsica. This picture is in agreement with the model proposed by Chemenda et al., (1996) for high compressional regime of continental subduction. In this model the crust failure was produced by high pressure and consequent high compressive stresses within the crust in front of the subduction zone. This implies the reduction of the compressive stresses in the front of the subduction, allowing the buoyancy forces to act on the subducted continental crust, which is forced to exhume. In this model, the ductile exhumation of continental metamorphic units was driven by the simultaneous activation of a thrusting system at their base and an extensional fault system at their top (i.e. at the base of the orogenic wedge represented by the Schistes Lustrés complex and the Upper Units).

Considering that the geothermal gradient estimated during the D2 deformation phase ($26.4^\circ\text{--}34.4^\circ\text{C/km}$) is greater respect the geothermal gradient calculated for the D1 phase ($6.3^\circ\text{--}25.9^\circ\text{C/km}$), we propose that the early exhumation of the Piedigriggio-Prato Unit took place in a period of transition from continental subduction to continental collision. If the D2 phase can be regarded as developed during the exhumation, it is important to underline how this tectonics is able both to partially obliterate the pre-existing fabric and, at the same time, to produce map-scale structures, previously interpreted as the result of the accretion processes of continental slices at the orogenic wedge (e.g. Egal, 1992).

A **completely** different picture arises from the D3 phase. Open to close F3 folds with sub-horizontal axial plane and the associated low-angle shear zones could be produced by vertical shortening of pre-existing non-horizontal layers during an extensional tectonics (**Fig. 12**) caused by the gravitational collapse of over-thickened continental crust (e.g. Froitzheim, 1992). However, the D3 structures can be also coherent with the back thrusting coeval with the activity of main frontal

thrusting towards the internal part of the orogenic wedge, that mark the end of continental subduction and the start of continental collision in the Western Alps (e.g. Freeman *et al.*, 1997). Regardless its geodynamic interpretation, the D3 phase was strictly connected with the emplacement of the Piedigrioglio-Prato Unit at very shallow structural levels ($T < 200^{\circ}\text{C}$) before the deposition of the Miocene deposits.

Our reconstruction for the evolution of the Piedigrioglio-Prato Unit fits very well with the models proposed for the exhumation of the continental high-pressure units of Alpine Corsica. For instance, Jolivet *et al.* (1991) have shown that at the end of Eocene time the compression stopped switching to widespread extensional tectonics involving crustal scale boudinage with the activation of east-verging, low-angle shear zones. In addition, Malavieille *et al.*, (1998) have proposed a model where the exhumation of oceanic and continental, high-pressure metamorphic fragments occurred since Late Cretaceous by extrusion tectonics driven by the buoyancy of the subducted continental crust. The same model has been proposed for the Tenda Massif by Molli *et al.* (2006) and Molli (2008) but with different timing for the extrusion (i.e. Middle to Late Eocene). Later, Rossetti *et al.*, (2015) provided an analogous picture where the transition from compression to extension in Alpine Corsica is documented as Late Oligocene–Early Miocene in age.

6. CONCLUSIONS

The micro- to map-scale structural analyses coupled with detailed metamorphic and thermodynamic investigations allow to reconstruct the evolution of the Piedigrioglio-Prato Unit during the syn-convergence-related processes. The involvement of this unit in the continental subduction processes is initially suggested by the unconformity at the top of the Triassic-Early Jurassic succession. The emplacement of these foredeep deposits (i.e. Metabreccias and Metaturbidites Fm.) in the Middle – Late Eocene, in fact, are related to the extensional deformation that affected the forebulge. The most important evidence for its involvement in the continental subduction, however, is provided by the new structural and metamorphic data provided by this study. The deformation history acquired during the exhumation path by the Piedigrioglio-Prato Unit consists of three phases (D1, D2, D3). The D1 and D2 deformation phases developed under retrograde P-T metamorphic conditions in a setting where the geothermal gradients increased from $6.3^{\circ}/25.9^{\circ}\text{C}/\text{km}$ to $26.4^{\circ}/34.4^{\circ}\text{C}/\text{km}$. Moreover, the structural features and the estimated P-T conditions suggest that the D1 and D2 phases were acquired during ductile extrusion active in a contest of transition from continental subduction to continental collision. Differently from the previously proposed reconstructions (Bezert and Caby 1988; Molli *et al.*, 2006; Malasoma and

Marroni, 2007; Molli, 2008), no evidence of prograde metamorphic evolution was recorded in the studied rocks. The D3 phase produced the last stages of exhumation up to the surface.

On the whole, the Piedigiglio-Prato Unit can be regarded as a reference for the exhumation of a continental fragments during a crucial period of the Alpine belt that corresponds to the transition from the continental subduction to continental collision. This transition is underlined by a ductile exhumation by extrusion tectonics of subducted continental crust in a frame of progressive change of geothermal gradient.

Acknowledgements

We would like to thank Giovanni Capponi and Alberto Vitale Brovarone for their constructive reviews. We are also thankful to the University of Pisa and the Institute des Science de la Terre of Grenoble for financial support of this project. The ERASMUS placement project provided the support for the collaboration between authors.

REFERENCES

- Alessandri, J.A., MagnA, J., Pilot, M.D., Samuel, E. 1977. Le Miocène de la region de Corte-Francardo. *Bulletin de la Societi Sciences Historiques et Naturelles de la Corse* **622**, 51-54.
- Amaudric Du Chaffaut, S. 1975. L'unité de Corte: un témoin de "Piémontais externe" en Corse? *Bulletin de la Societi GéGcietin de France* **7**, 739-745.
- Bezert, P., Caby, R. 1988. Sur l'âge post-bartonien des événements tectono-métamorphiques alpins en bordure orientale de la Corse cristalline (Nord de Corte). *Bulletin de la Societi Géocietin de France* **4(6)**, 965-971.
- Boccaletti, M., Elter, P., Guazzone, G. 1971. Plate tectonic models for the development of the western Alps and northern Apennines. *Nature* **234**, 108-111.
- Bourdelle, F., Parra, T., Chopin, C., Beyssac., O. 2013. A new chlorite geothermometer for diagenetic to low-grade metamorphic conditions. *Contributions to Mineralogy and Petrology* **165**, 723-735.
- Brun, J.P., Faccenna, C. 2008. Exhumation of high-pressure rocks driven by slab rollback. *Earth and planetary Science Letters* **272**, 1-7.
- Brunet, C., Moniary SciJolivet, L., Cadet, J.P. 2000. Migration of compression and extension in the Tyrrhenian Sea, insights from $^{40}\text{Ar}/^{39}\text{Ar}$ ages on micas along a transect from Corsica to Tuscany. *Tectonophysics* **321**, 127-155.
- Burkhard, M. 1993. Calcite twins, their geometry, appearance and significance as stress-strain markers and indicators of tectonic regime: a review. *Journal of Structural Geology* **15**, 351- 368.
- Cabanis, B., CochemC, J.J., Vellutini, P.J., Joron, J.L., Treuil, M. 1990. Post-collisional Permian volcanism in northwestern Corsica: an assessment based on mineralogy and trace-element geochemistry. *Journal of Volcanology and Geothermal Research* **44**, 51-67.
- Caron, J.M., Delcey, R. 1979. Lithostratigraphie des Schistes Lustrés corses : diversité des series post-ophiolitiques. *Comptes Rendus de l'AcadAcad des Sciences* **288**, 1525-1528.
- Caron, J.M. 1994. Metamorphism and deformation in Alpine Corsica. *Schweizerische Mineralogische und Petrographische Mitteilungen* **74(1)**, 105-114.
- Cavazza, W., Zattin, M., Ventura, B., Zuffa, G.G. 2001. Apatite fission-track analysis of Neogene exhumation in northern Corsica (France). *Terranova* **13**, 51-57.
- Cathelineau, M., Nieva, D. 1985. A chlorite solid solution geothermometer. The Los Azufres (Mexico) geothermal system. *Contributions to Mineralogy and Petrology* **91**, 235-244.
- Cathelineau, M. 1988. Cation site occupancy in chlorites and illites as a function of temperature. *Clay minerals* **23**, 471-485.
- Chemenda, A.I., Mattauer, M., Malavieille, J., Bokun, A.N. 1995. A mechanism for syn-collisional deep rock exhumation and associated normal faulting: Results from physical modeling. *Earth and Planetary Science Letters* **132**, 225-232.

- 637 **Chemenda, A.I., Mattauer, M., Bokun, A.N. 1996.** Continental subduction and mechanism for exhumation
638 of high-pressure metamorphic rocks: new modelling and field data from Oman. *Earth and Planetary*
639 *Science Letters* **143**, 173-182.
- 640 **Chopin, C., Beyssac, O., Bernard, S., Malavieille, J. 2008.** Aragonite-grossular intergrowths in eclogite-
641 facies marble, Alpine Corsica. *European Journal of Mineralogy* **20**, 857-865.
- 642 **Cloos, M. 1982.** Flow melanges: Numerical modeling and geological constraints on their origin in the
643 Franciscan subduction complex. *Geological Society of America Bulletin* **93**, 330-345.
- 644 **Dallan, L., Nardi, R. 1984.** Ipotesi dell'evoluzione dei domini "liguri" della Corsica nel quadro della
645 paleogeografia e della paleotettonica delle unità. *Bollettino della Societ Geologica Italiana* **103**, 515-
646 527.
- 647 **Dallan, L., Puccinelli, A. 1995.** Geologia della regione tra Bastia e St. Florent (Corsica Settentrionale).
648 *Bollettino della Societ Geologica Italiana* **114**, 23-66.
- 649 **Daniel, J.M., Jolivet, L., Goff, B., Poinssot, C. 1996.** Crustal-scale strain partitioning: footwall
650 deformation below the Alpine Oligo-Miocene detachment of Corsica. *Journal of Structural Geology*
651 **18(1)**, 41-59.
- 652 **De Andrade, V., Vidal, O., Lewin, E., O'Brien, P., Agard, P. 2006.** Quantification of electron microprobe
653 compositional maps of rock thin sections: an optimized method and examples. *Journal of metamorphic.*
654 *Geology* **24**, 655-668.
- 655 **Dewey, J.F., Ryan, P.D., Andersen, T.B. 1993.** Orogenic uplift and collapse, crustal thickness, fabrics and
656 phase changes: the role of eclogites. In: *Magmatic processes and plate tectonics*, Prichard, H. M.,
657 Alabaster, T., Harris, N. B. W. & Neary, C. R. (eds), *Geological Society of London, Special Publication*
658 **76**, 325-343.
- 659 **Doglioni, C., Mongelli, F., Piali, G. 1998.** Boudinage of the Alpine belt in the Apenninic back-arc.
660 *Memorie della Societ Geologica Italiana* **52**, 457-468.
- 661 **Dubacq, B., Vidal, O., De Andrade, V. 2010.** Dehydration of dioctahedral aluminous phyllosilicates:
662 thermodynamic modelling and implications for thermobarometric estimates. *Contributions to*
663 *Mineralogy and Petrology* **159**, 159-174.
- 664 **Durand-Delga, M. 1984.** Principaux traits de la Corse Alpine et correlations avec les Alpes Ligures.
665 *Memorie della Societ Geologica Italiana* **28**, 285-329.
- 666 **Durand-Delga, M., Peybernée, B., Rossi, P. 1997.** Arguments en faveur de la position, au Jurassique, des
667 ophiolites de Balagne (Haute-Corse, France) au voisinage de la marge continentale europa. *Comptes*
668 *Rendus de l'Acad Acad des Sciences* **325**, 973-981.
- 669 **Egal, E. 1992.** Structures and tectonic evolution of the external zone of Alpine Corsica. *Journal of Structural*
670 *Geology* **14**, 1215-1228.
- 671 **Faure, M., Malavieille, J. 1981.** Étude structurale d'un cisaillement ductile: le charriage ophiolitique corse
672 dans la region de Bastia. *Bulletin de la Société Géologique de France* **23(4)**, 335-343.
- 673 **Fellin, M.G., Picotti, V., Zattin, M. 2005.** Neogene to Quaternary rifting and inversion in Corsica: Retreat
674 and collision in the western Mediterranean. *Tectonics* **24**, TC1011, doi:10.1029/2003TC001613.

- 675 **Ferrandini, M., Ferrandini, J., Loyer-Pilot, M.D., Butterlin, J., Cravatte, J., Janin, M.C. 1998.** Le
676 Miocène du bassin de Saint-Florent (Corse): modalités de la transgression du Burdigalien supérieur et
677 mise en évidence du Serravallien. *Geobios* **31**(1), 125-137.
- 678 **Ferrandini, J., Gattacceca, J., Ferrandini, M., Deino, A., Janin, M.C. 2003.** Chronostratigraphie et
679 paléomagnétisme des dépôts oligo-miocènes de Corse: implications géodynamique pour l'ouverture du
680 bassin liguro-provençal. *Bulletin de la Société Géologique de France* **174**(4), 357-371.
- 681 **Ford, M., Lickorish, W.H., Kuszniir, N.J. 1999.** Tertiary foreland sedimentation in the Southern Subalpine
682 Chains, SE France: a geodynamic appraisal. *Basin Research* **11**, 315-336.
- 683 **Fournier, M., Jolivet, L., Goffé, B., Dubois R. 1991.** The Alpine Corsica metamorphic core complex.
684 *Tectonics* **10**(6), 1173-1186.
- 685 **Freeman, S.R., Inger, S., Butler, R.W., Cliff, R.A. 1997.** Dating deformation using Rb-Sr in white mica:
686 greenschist facies deformation ages from Entrelor shear zone, Italian Alps. *Tectonics* **16**(1), 57-76.
- 687 **Froitzheim, N., 1992.** Formation of recumbent folds during synorogenic crustal extension (Austroalpine
688 nappes, Switzerland). *Geology* **20**, 923-926.
- 689 **Ganne, J., Bertrand, J.M., Fudral, S., Marquer, D., Vidal, O. 2007.** Structural and metamorphic
690 evolution of the Ambin massif (western Alps): toward a new alternative exhumation model for the
691 Briançonnais domain. *Bulletin de la Société Géologique de France* **178**, 437-458.
- 692 **Garfagnoli, F., Menna, F., Pandeli, E., Principi, G. 2009.** Alpine metamorphic and tectonic evolution of
693 the Inzecca - Ghisoni area (southern Alpine Corsica, France). *Geological Journal* **44**, 191-210.
- 694 **Gibbons, W., Horak, J. 1984.** Alpine metamorphism of Hercynian hornblende granodiorite beneath the
695 blueschist facies Schistes Lustrés nappe of NE Corsica. *Journal of Metamorphic Geology* **2**, 95-113.
- 696 **Gibbons, W., Waters, C., Warburton, J. 1986.** The blueschist facies Schistes Lustrés of Alpine Corsica: a
697 review. *Geological Society of America Memoir* **164**, 301-331.
- 698 **Gradstein, F.M., Ogg, J.G., Schmitz, M.D. 2012.** *The Geologic Time Scale 2012*. Boston, USA, Elsevier,
699 DOI: 10.1016/B978-0-444-59425-9.00004-4.
- 700 **Gueguen, E., Doglioni, C., Fernandez, M. 1998.** On the post-25 Ma geodynamic evolution of the western
701 Mediterranean. *Tectonophysics* **298**, 259-269.
- 702 **Guillot, S., Hattori, K., De Sigoyer, J., Nagler, T., Auzende, A.L. 2001.** Evidence of hydration of the
703 mantle wedge and its role in the exhumation of eclogites. *Earth Planetary Science Letters* **193**, 115-127.
- 704 **Guillot, S., Hattori, K., Agard, P., Schwartz, S., Vidal, O. 2009.** Exhumation processes in oceanic and
705 continental subduction context: A Review. In: *Subduction zone geodynamics*, Lallemand, S., Funiciello,
706 F., (eds.), Frontiers in Earth Sciences, Springer, DOI 10.1007/978-3-5.
- 707 **Handy, M.R., Schmid, S.M., Bousquet, R., Kissling, E., Bernoulli, D. 2010.** Reconciling plate-tectonic
708 reconstructions of Alpine Tethys with the geological-geophysical record of spreading and subduction in
709 the Alps. *Earth Science Reviews* **102**, 121-158.
- 710 **Harris, L. 1985.** Progressive and polyphase deformation of the Schistes Lustrés in Cap Corse, Alpine
711 Corsica. *Journal of Structural Geology* **7**(6), 637-650.
- 712 **Hillier, S., Velde, B. 1991.** Octahedral occupancy and the chemical composition of diagenetic

- (low-temperature) chlorites. *Clay Minerals* **26**, 146-168.
- Jolivet, L., Dubois, R., Fournier, M., Goffé, B., Michard, A., Jordan, C. 1990. Ductile extension in Alpine Corsica. *Geology* **18**, 1007-1010.
- Jolivet, L., Daniel, J.M., Fournier, M. 1991. Geometry and Kinematics of ductile extension in Alpine Corsica. *Earth and Planetary Science Letters* **104**, 278-291.
- Jolivet, L., Faccenna, C., Goffé, B., Burov, E., Agard, P. 2003. Subduction tectonics and exhumation of high-pressure metamorphic rocks in the Mediterranean orogens. *American Journal of Science* **303**, 353-409.
- Lacombe, O., Jolivet, L. 2005. Structural and kinematic relationships between Corsica and the Pyrenees-Provence domain at the time of the Pyrenean orogeny. *Tectonics* **24**, TC1003, doi:10.1029/2004TC001673.
- Lahondère, D., Guerrot, C. 1997. Datation Sm-Nd du métamorphisme éclogitique en Corse alpine: un argument pour l'existence au Crétacé supérieur d'une zone de subduction active localisées sous le bloc corso-sarde. *Géologie de la France* **3**, 3-11.
- Lanari, P., Guillot, S., Schwartz, S., et al. 2012. Diachronous evolution of the alpine continental subduction wedge: Evidence from P-T estimates in Briançonnais zone houillère (France-Western Alps). *Journal of Geodynamics* **56-57**, 39-54.
- Lanari, P., Rolland, Y., Schwartz, S., et al. 2014. P-T-t estimation of deformation in low-grade quartz-feldspar-bearing rocks using thermodynamic modelling and $^{40}\text{Ar}/^{39}\text{Ar}$ dating techniques: example of the Plan-de-Phasy shear zone unit (Briançonnais zone, Western Alps). *Terra Nova* **26**, 130-138.
- Laporte, D., Fernandez, A., Orsini, J.B. 1991. Le complexe d'Ile Rousse, Balagne, Corse du Nord-Ouest: pétrologie et cadre de mise en place des granitoides magnésio-potassiques. *Geologie de la France* **4**, 15-30.
- Levi, N., Malasoma, A., Marroni, M., Pandolfi, L., Paperini, M. 2007. Tectono- metamorphic history of the ophiolitic Lento unit (northern Corsica): evidences for the complexity of accretion-exhumation processes in a fossil subduction system. *Geodinamica Acta* **20(1)**, 99-118.
- Maggi, M., Rossetti, F., Corfu, F., et al. 2012. Clinopyroxene-rutile phyllonites from East Tenda Shear Zone (Alpine Corsica, France): pressure-temperature-time constraints to the Alpine reworking of Variscan Corsica. *Journal of the Geological Society of London*, **169**, 723-732.
- Malasoma, A., Marroni, M., Musumeci, G., Pandolfi, L. 2006. High-pressure mineral assemblage in granitic rocks from continental units, Alpine Corsica, France. *Geological Journal* **41**, 49-59.
- Malasoma, A., Marroni, M. 2007. HP/LT metamorphism in the Volparone Breccia (Northern Corsica, France): evidence for involvement of the Europe/Corsica continental margin in the Alpine subduction zone. *Journal of Metamorphic Geology* **25**, 529-545.
- Malavieille, J., Chemenda, A., Larroque, C. 1998. Evolutionary model for the Alpine Corsica: mechanism for ophiolite emplacement and exhumation of high-pressure rocks. *Terra Nova* **10**, 317-322.

- 749 **Maluski, H. 1977.** *Application de la méthode $^{40}\text{Ar}/^{39}\text{Ar}$ aux minéraux des roches cristallines perturbées par*
 750 *des événements thermiques et tectoniques en Corse.* PhD thesis, University of Montpellier.
- 751 **Marroni, M., Pandolfi, L. 2001.** Debris flow and slide deposits at the top of the Internal Liguride ophiolitic
 752 sequence (Northern Apennine, Italy): a record of frontal tectonic erosion in a fossil accretionary wedge.
 753 *The Island Arc* **10**, 9-21.
- 754 **Marroni, M., Pandolfi, L. 2003.** Deformation history of the ophiolite sequence from the Balagne Nappe,
 755 northern Corsica: insights in the tectonic evolution of the Alpine Corsica. *Geological Journal* **38(1)**, 67-
 756 83.
- 757 **Marroni, M., Pandolfi, L. 2007.** The architecture of an incipient oceanic basin: a tentative reconstruction of
 758 the Jurassic Liguria- Piemonte basin along the Northern Apennine - Alpine Corsica transect.
 759 *International Journal of Earth Science* **96**, 1059-1078.
- 760 **Marroni M., Meneghini F., Pandolfi L. 2010.** Anatomy of the Ligure-Piemontese subduction system:
 761 evidence from Late Cretaceous-Middle Eocene convergence-related deposits from Northern Apennines
 762 (Italy). *International Geology Review* **10-12**, 1160-1192.
- 763 **Martin, A.J., Rubatto, D., Vitale Brovarone, A., Hermann, J. 2011.** Late Eocene lawsonite-eclogite
 764 facies metasomatism of a granulite sliver associated to ophiolites in Alpine Corsica. *Lithos* **125**, 620-
 765 640.
- 766 **Massonne, H.J., Schreyer, W. 1987.** Phengite geobarometry based on the limiting assemblage with K-
 767 feldspar, phlogopite, and quartz. *Contributions to Mineralogy and Petrology* **96**, 212-224.
- 768 **Massonne, H.J., Szpurka, Z. 1997.** Thermodynamic properties of white micas on the basis of high-pressure
 769 experiments in the systems $\text{K}_2\text{MgO-Al}_{23}\text{SiO}_2\text{H}_2$ and $\text{K}_2\text{FeO-Al}_{23}\text{SiO}_2\text{H}_2$. *Lithos* **41**, 229-250.
- 770 **Massonne, H.J. 1998.** Ultra-high pressure metamorphism of rocks from the Gneiss-Eclogite Unit of the
 771 Saxonian Erzgebirge, Germany. *Transactions American Geophysical Union* **79**, 24-129.
- 772 **Mattauer, M., Proust, F. 1976.** La Corse alpine: un modèle de genèse du métamorphisme haute pression
 773 par subduction de croûte continentale sous du matériel océanique. *Compte Rendu de l'Académie des*
 774 *Sciences*, Paris, **282**, 1249-1252.
- 775 **Mattauer, M., Faure, M., Malavieille, J. 1981.** Transverse lineation and large scale structures related to
 776 Alpine obduction in Corsica. *Journal of Structural Geology*, **3**, 401-409.
- 777 **Mattauer, M., Proust, F., Etchecopar, A. 1977.** Linéation "a" et mécanisme de cisaillement simple liés au
 778 chevauchement de la nappe de schistes lustrés en Corse. *Bulletin de la Société Géologique de la France*
 779 **14**, 841-945.
- 780 **Mauffret, A., Contrucci, I., Brunet, C. 1999.** Structural evolution of the northern Tyrrhenian Sea from new
 781 seismic data. *Marine and Petroleum Geology* **16**, 381-407.
- 782 **Ménot, R.P. 1990.** Evolution du socle anté-Stéphanien de Corse. *Schweizerische mineralogische und*
 783 *petrographische mitteilungen* **70**, 35-54.
- 784 **Michard, A., Martinotti, G. 2002.** The Eocene unconformity of the Briançonnais domain in the French-
 785 Italian Alps, revisited (Margaritis massif, Cuneo); a hint for a Late Cretaceous-Middle Eocene frontal
 786 bulge setting. *Geodinamica Acta* **15**, 289-301.

- 787 **Molli, G., Tribuzio, R. 2004.** Shear zones and metamorphic signature of subducted continental crust as
 788 tracers of the evolution of the Corsica/Northern Apennine orogenic system. In: *Flow processes in faults*
 789 *and shear zones*, Alsop, G.I., Holdsworth, R.E., McCaffrey, K.J.W., Handy, M. (eds), Geological
 790 Society, London, Special Publications, **224**, 321-335.
- 791 **Molli, G., Tribuzio, R., Marquer, D. 2006.** Deformation and metamorphism at the eastern border of Tenda
 792 Massif (NE Corsica): a record of subduction and exhumation of continental crust. *Journal of Structural*
 793 *Geology*, **28**, 1748-1766.
- 794 **Molli, G. 2008.** Northern Apennine-Corsica orogenic system: an updated overview. In: *Tectonic Aspects of*
 795 *the Alpine-Dinaride-Carpathian System*, Siegesmund S, FS, Fsmund B, Froitzheim N (eds.), The
 796 Geological Society of London, Special Publication **298**, 413 - 442.
- 797 **Molli, G., Malavieille, J. 2011.** Orogenic processes and the Corsica/Apennines geodynamic evolution:
 798 insights from Taiwan. *International Journal of Earth Sciences* **100**, 1207-1224.
- 799 **Oberhänsli, R., Bousquet, R., Engi, M., et al. 2004.** *Metamorphic structure of the Alps*. Commission for
 800 the Geological Map of the World, Paris, scale 1:1.000.000.
- 801 **Padoa, E., Saccani, E., Durand-Delga, M. 2001.** Structural and geochemical data on the Rio Magno Unit:
 802 evidences for a new new on the Rio Magno Unit: evidences for a new from Taiwations. *Terra Nova*
 803 **13**, 135-142.
- 804 **Pandolfi, L., Marroni, M., Malasoma, A. 2016.** Stratigraphic and structural features of the Bas-Ostriconi
 805 unit (Corsica): paleogeographic implications. *Compte Rendu Geoscience*, in press.
- 806 **Paquette, J.L., Maqot, R.P., Pin, C., Orsini, J.B. 2003.** Episodic and short-lived granitic pulses in a post-
 807 collisional setting: evidence from precise U-Pb zircon dating through a crustal cross-section in Corsica.
 808 *Chemical Geology* **198**, 1-20.
- 809 **Parra, T., Vidal, O., and Agard, P. 2002.** A thermodynamic model for Fe-Mg dioctahedral K white micas
 810 using data from phase-equilibrium experiments and natural pelitic assemblages. *Contribution to*
 811 *Mineralogy and Petrology* **143**, 706-732.
- 812 **Platt, J.P. 1986.** Dynamics of orogenic wedges and the uplift of high-pressure metamorphic rocks.
 813 *Geological Society of America Bulletin* **97(9)**, 1037-1053.
- 814 **Ramsay, J.G. 1967.** *Folding and fracturing of rocks*. McGraw-Hill: New York.
- 815 **Ravna, E.J.K., Andersen, T.B., Jolivet, L., De Capitani, C. 2010.** Cold subduction and the formation of
 816 lawsonite eclogite – from prograde evolution of eclogitized pillow lava from Corsica. *Journal of*
 817 *Metamorphic Geology* **28**, 381-395.
- 818 **Ritsema, L. 1952.** *Géologie de la region de Corte (Corse)*. PhD thesis, University of Amsterdam.
- 819 **Rossetti, F., Glodny, J., Theye, T., Maggi, M. 2015.** Pressure-temperature-deformation-time of the ductile
 820 Alpine shearing in Corsicare From orogenic construction to collapse. *Lithos* **218-219**, 99-116.
- 821 **Rossi, P., Durand-Delga, M., Caron, J.M., et al. 1994.** *Notice explicative de la Feuille Corte*. Editions du
 822 BRGM, scale 1/50,000.

- 823 **Rossi, P., Cocherie, A., LahondLre, D., Fanning, C.M. 2002.** La marge européenne de la Téthys
 824 jurassique en Corse: datation de trondhjémites de Balagne et indices de croûte continentale sous le
 825 domaine Balano-Ligure. *Comptes Rendus Geoscience* **334** 313-322.
- 826 **Rossi, P., Oggiano, G., Cocherie, A. 2009.** A restored section of the “southern Variscan realm” across the
 827 Corsica-Sardinia microcontinent. *Comptes Rendus Geoscience* **341(2-3)**, 224-238.
- 828 **Saccani, E., Padoa, E., Tassinari, R. 2000.** Preliminary data on the Pineto gabbroic massif and Nebbio
 829 basalts: progress toward the geochemical characterization of alpine Corsica ophiolites. *Ophioliti* **25**, 75-
 830 86.
- 831 **Sagri, M., Aiello, E., Certini, L. 1982.** Le unità torbiditiche cretacee della Corsica. *Rendiconti della Società*
 832 *Geologica Italiana* **5**, 87-91.
- 833 **Schmid, S.M., Pfiffner, O.A., Froitzheim, N., Schonborn, G., Kissling, E. 1996.** Geophysical-geological
 834 transect and tectonic evolution of Swiss-Italian Alps. *Tectonics* **15(5)**, 1036-1064.
- 835 **Sinclair, H.D. 1997.** Tectonostratigraphic model for underfilled peripheral foreland basins: an Alpine
 836 perspective. *Geological Society of American Bulletin* **109(3)**, 324-346.
- 837 **Stampfli, G.M., Mosar, J., Marquer, D., Marchant, R., Baudin, T., Borel, G., 1998.** Subduction and
 838 obduction processes in the Swiss Alps. *Tectonophysics* **296**, 159-204.
- 839 **Steck, A., Epard, J.L., Vannay, J.C., et al. 1998.** Geological transect across the Tso Moriri and Spiti areas:
 840 the nappe structures of the Tethys Himalaya. *Eclogae Geologicae Helvetiae* **91**, 103-121.
- 841 **Thompson, A.B., Schulmann, K., Jezek, J. 1997.** Thermal evolution and exhumation in obliquely
 842 convergent (transpressive) orogens. *Tectonophysics* **280**, 171-184.
- 843 **Tribuzio, R., Giacomini, F. 2002.** Blueschist facies metamorphism of peralkaline rhyolites from Tenda
 844 crystalline massif (northern Corsica): evidence for involvement in the Alpine subduction event? *Journal*
 845 *of Metamorphic Geology* **20**, 513-526.
- 846 **Velde, B. 1965.** Phengitic micas: Synthesis, stability, and natural occurrence. *American Journal of Science*
 847 **263**, 886-913.
- 848 **Vidal, O., Parra, T. 2000.** Exhumation paths of high-pressure metapelites obtained from local equilibria for
 849 chlorite-phengite assemblage. *Geological Journal* **35**, 139-161.
- 850 **Vidal, O., De Andrade, V., Lewin, E., Munoz, M., Parra, T., Pascarelli, S. 2006.** P-T deformation
 851 $\text{Fe}^{2+}/\text{Fe}^{3+}$ mapping at the thin section scale and comparison with XANES mapping: application to a
 852 garnet-bearing metapelite from the Sambagawa metamorphic belt (Japan). *Journal of Metamorphic*
 853 *Geology* **24**, 669-683.
- 854 **Vitale Brovarone, A., Groppo, C., Hetényi, H. R., Compagnoni, R., Malavieille, J. 2011.** Coexistence of
 855 lawsonite-bearing eclogite and blueschist: phase equilibria modelling of Alpine Corsica metabasalts and
 856 petrological evolution of subducting slabs. *Journal of Metamorphic Geology* **29**, 583-600.
- 857 **Vitale Brovarone, A., Herwartz, D. 2013.** Timing of HP metamorphism in the Schistes Lustrés of Alpine
 858 Corsica: new Lu-Hf garnet and lawsonite ages. *Lithos* **172-173t**, 175-191.

- 859 **Vitale Brovarone, A., Beyssac, O., Malavieille, J., Molli, G., Beltrando, M., Compagnoni, R. 2013.**
860 Stacking and metamorphism of continuous segments of subducted lithosphere in a high-pressure wedge:
861 The example of Alpine Corsica (France). *Earth-Science Reviews* **116**, 35-56.
- 862 **Warburton, J. 1986.** The ophiolite-bearing Schistes Lustrés segments of subducted lithosphere in a
863 emplacement of ophiolites that have suffered HP/LT metamorphism. *Geological Society of America*
864 *Memoirs* **164**, 313-331.
- 865 **Waters, C.N. 1990.** The Cenozoic tectonic evolution of Alpine Corsica. *Journal of Geological Society of*
866 *London* **147**, 811-824.
- 867 **Zarki-Jakni, B., Van Der Beek, P., Poupeau, G., Sosson, M., Labrin, E., Rossi, P., Ferrandini, J. 2004.**
868 Cenozoic denudation of Corsica in response to Ligurian and Tyrrhenian extension: Results from apatite
869 fission track thermochronology. *Tectonics* **23**, TC1003, doi:10.1029/2003TC001535.

CAPTIONS

Figure 1 Geological setting of the study area. (A) Tectonic sketch-map of the Alpine Corsica (the study-area is highlighted in red) and related geological cross-section (from Malavieille *et al.*, 1998, modified). MQd: Miocene and Quaternary deposits (F: Francardo basin, SF: Saint-Florent Basin); UU: Upper Units (Ne: Nebbio Unit, Ba: Balagne Unit, P: Pineto Unit, SLu: Santa Lucia Unit); SL: Schistes Lustrés (dashed line indicates the trace of the foliation); LU: Lower Units (Ce: Centuri Unit, Pi: Serra di Pigno Unit, Tm: Tenda massif, CU: Corte Units, UC: Caporalino Unit); Usc: Eocene unmetamorphosed sedimentary cover; Hb: Hercynian basement; CCSZ: Central Corsica Shear Zone. (B) Tectonic sketch map of the area between Francardo, Castirla and Corte (black square indicates the study area). The relationship between the Hercynian basement, the Lower Units, here represented by the Corte Units, i.e. Popolasca-Castiglione Unit (UPC), Croce d'Arbitro Unit (UCA), Piedigriggio-Prato Unit (UPP), the Caporalino Unit (UC) and the Schistes Lustrés are shown (Qd: quaternary deposits).

Figure 2. Geological map of the Monte Cecu area and related geological cross-section. The locations of the two studied samples (CM21 and CM32) are also indicated. RB: Roches Brunes Fm., Mv: Metavolcanites and Metavolcanoclastites Fm., Md: Metadolomites Fm., Mc: Metaconglomerates Fm., MM: Metalimestones and Metadolomites Fm., LM: Lumachella Metalimestones Fm., TM: Thin-bedded Metalimestones Fm., CM: Cherty Metalimestones Fm., DM: Detritic Metalimestones Fm., Mb: Metabreccias Fm., Mt: Metaturbidites Fm., Mba: Metabasalts Fm., Qd: Quaternary deposits.

Figure 3. Reconstruction of the complete stratigraphic log of the Piedigriggio - Prato Unit by integration of stratigraphic data from the study and the neighbouring areas. RB: Roches Brunes Fm., Mg: Metagranites Fm., Mv: Metavolcanites and Metavolcanoclastites Fm., Md: Metadolomites Fm., Mc: Metaconglomerates Fm., MM: Metalimestones and Metadolomites Fm., LM: Lumachella Metalimestones Fm., TM: Thin-bedded Metalimestones Fm., CM: Cherty Metalimestones Fm., DM: Detritic Metalimestones Fm., Mb: Metabreccias Fm., Mt: Metaturbidites Fm.

Figure 4. (A) F2 fold in Metaturbidites Fm. deforming lithological boundary, graded bedding and S1 foliation. (B) Metabreccias Fm. hand-sample showing high-ratio x:z flattened clasts. (C) Fractured porphyroclast wrapped by the S2 foliation in the Metabreccias Fm. (thin section, crossed nicols); (D) Crystals of calcite with type-2 twins in the Metabreccias Fm. (thin section, crossed nicols). (E) Relationship between S1 and S2 foliations in the matrix of the Metabreccias Fm. (thin

section, crossed nicols). (F) S3 crenulation cleavage in the pelitic matrix of Metabreccias Fm. (I) F3 fold in Detritic Metalimestones Fm. (thin section, crossed nicols).

Figure 5. Stereographic plots of structural data collected in the study area (Schmidt net projection, lower hemisphere) and related schematic model of the folding. Density classes: 1% contour.

Figure 6. Si/XMg plot for chlorites (A) and Si/Al plot for phengites (B) of the studied samples.

Figure 7. (A) Quantitative histogram of chlorites in equilibrium at different temperatures for sample CM21. (B) Temperature vs. Fe^{3+} plot from the chlorites in sample CM32.

Figure 8. P-T equilibria conditions obtained with the application of the Chlorite-Phengite-Quartz-Water multiequilibrium approach on the CM21 and CM32C samples.

Figure 9. (A) Ternary diagram of phengite end-members for sample CM21 (XMu: muscovite, XCel: celadonite, XPyr: pyrophyllite). Red points: phengites more enriched in the muscovitic end-member grown along the S1 foliation. Blue points: phengites enriched in the celadonitic end-member grown in the S2 foliation. (B) P-T path showing the equilibria conditions obtained for phengites plotted in (A). (C) Element map showing the phengites grew during the D1 phase (in red) and the D2 phase (in blue).

Figure 10. (A) Si-intensity map acquired with EPMA (sample CM21); five phases are identifiable: quartz (level 17395-11968), feldspar (level 11968-10000), phengite (level 10000-6500), chlorite (6500-3000). (B) P-T equilibria conditions of sample CM21. Arrows indicate the studied areas.

Figure 11. P-T-d path obtained for sample CM32C; the crosses indicate the P-T conditions calculated for the chlorite-phengite couples grew equilibria during the D1 and D2 phases. The dash lines at $T = 200^\circ\text{C}$ indicate the deformation temperature estimated for the D3 phase using calcite twins.

Figure 12. (A) Cartoon illustrating the tectono-metamorphic evolution of the Piedigrioglio-Prato Unit (indicated with the star) during the Late Eocene-Oligocene time span. From the top of the bottom: underthrusting of the Piedigrioglio-Prato Unit at depth of 30 km into the orogenic wedge during the D1 phase, followed by the onset of the exhumation; continuous exhumation during the D2 phase from ~ 30 km to ~ 10 km of depth; final stage of exhumation produced by extensional

1
2 942 tectonics driven by low-angle normal faults during the D3 phase. (B) P-T-d path elaborated for the
3 943 Piedigrioglio-Prato Unit.
4
5 944
6
7 945
8 946 TABLES
9
10 947
11 948 Table 1. Maximum temperature (°C) estimates obtained using different different geothermometers.
12
13 949
14
15 950 Table 2. Pressure (kbar) estimates obtained using the Massonne and Schreyer geobarometer (1988).
16
17 951
18 952 Table 3. Representative electron microprobe analyses of the chlorite-phengite pairs of the
19
20 953 Metabreccias Fm.
21
22 954
23
24
25
26
27
28
29
30
31
32
33
34
35
36
37
38
39
40
41
42
43
44
45
46
47
48
49
50
51
52
53
54
55
56
57
58
59
60

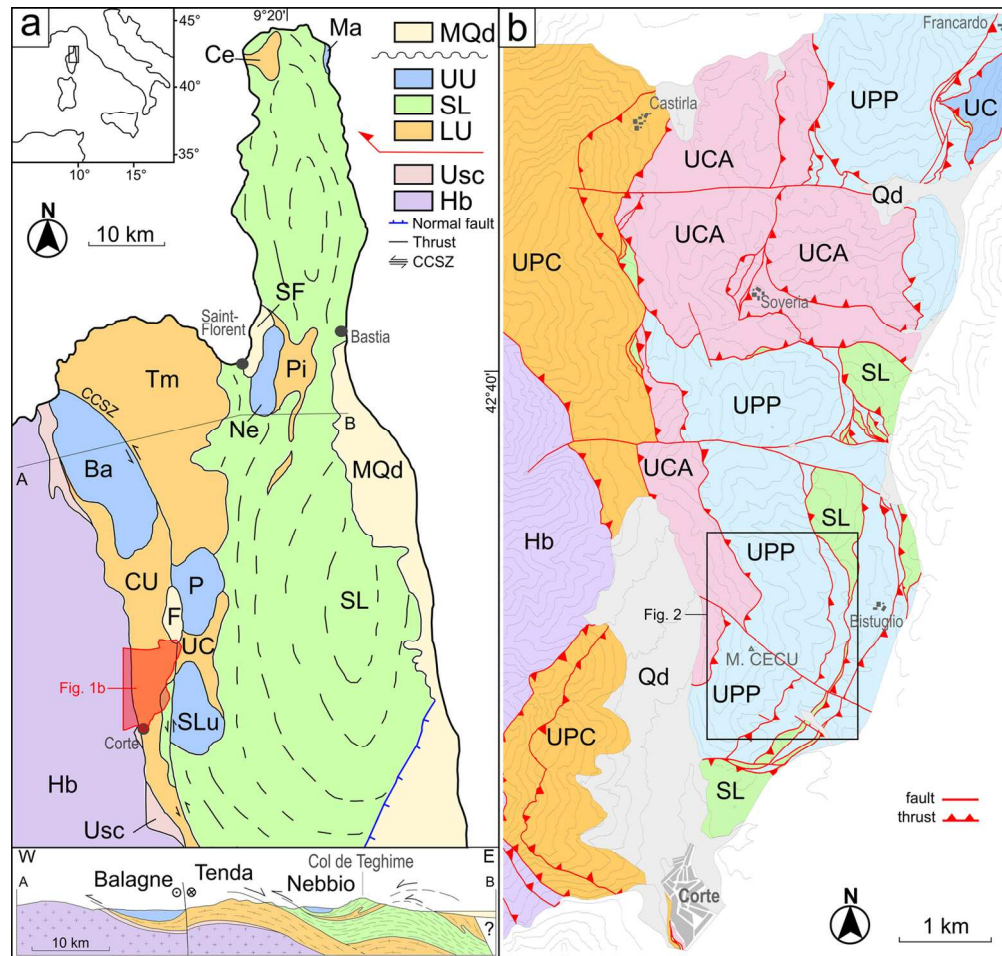


Figure 1 Geological setting of the study area. (A) Tectonic sketch-map of the Alpine Corsica (the study-area is highlighted in red) and related geological cross-section (from Malavielle et al., 1998, modified). MQd: Miocene and Quaternary deposits (F: Francardo basin, SF: Saint-Florent Basin); UU: Upper Units (Ne: Nebbio Unit, Ba: Balagne Unit, P: Pineto Unit, SLu: Santa Lucia Unit); SL: Schistes Lustrés (dashed line indicates the trace of the foliation); LU: Lower Units (Ce: Centuri Unit, Pi: Serra di Pigno Unit, Tm: Tenda massif, CU: Corte Units, UC: Caporalino Unit); Usc: Eocene unmetamorphosed sedimentary cover; Hb: Hercynian basement; CCSZ: Central Corsica Shear Zone. (B) Tectonic sketch map of the area between Francardo, Castirla and Corte (black square indicates the study area). The relationship between the Hercynian basement, the Lower Units, here represented by the Corte Units, i.e. Popolasca-Castiglione Unit (UPC), Croce d'Arbitro Unit (UCA), Piedigriggio-Prato Unit (UPP), the Caporalino Unit (UC) and the Schistes Lustrés are shown (Qd: quaternary deposits).

142x135mm (300 x 300 DPI)

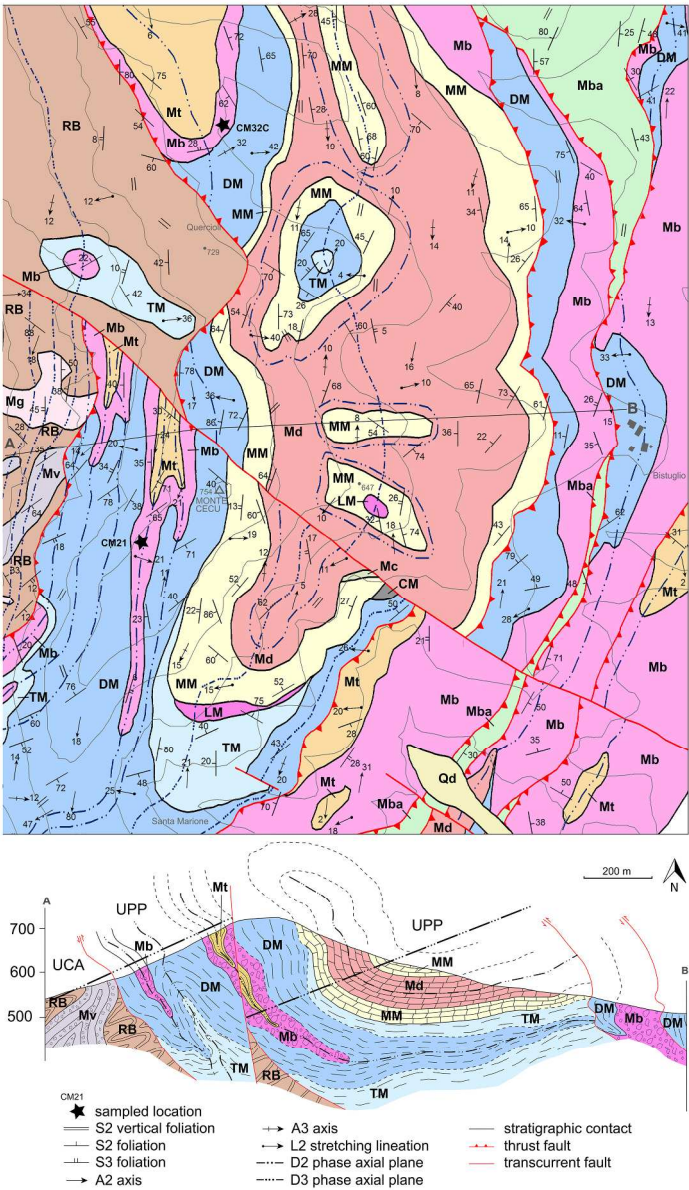


Figure 2. Geological map of the Monte Cecu area and related geological cross-section. The locations of the two studied samples (CM21 and CM32) are also indicated. RB: Roches Brunes Fm., Mv: Metavolcanites and Metavolcanoclastites Fm., Md: Metadolomites Fm., Mc: Metaconglomerates Fm., MM: Metalimestones and Metadolomites Fm., LM: Lumachella Metalimestones Fm., TM: Thin-bedded Metalimestones Fm., CM: Cherty Metalimestones Fm., DM: Detritic Metalimestones Fm., Mb: Metabreccias Fm., Mt: Metaturbidites Fm., Mba: Metabasalts Fm., Qd: Quaternary deposits.

250x428mm (300 x 300 DPI)

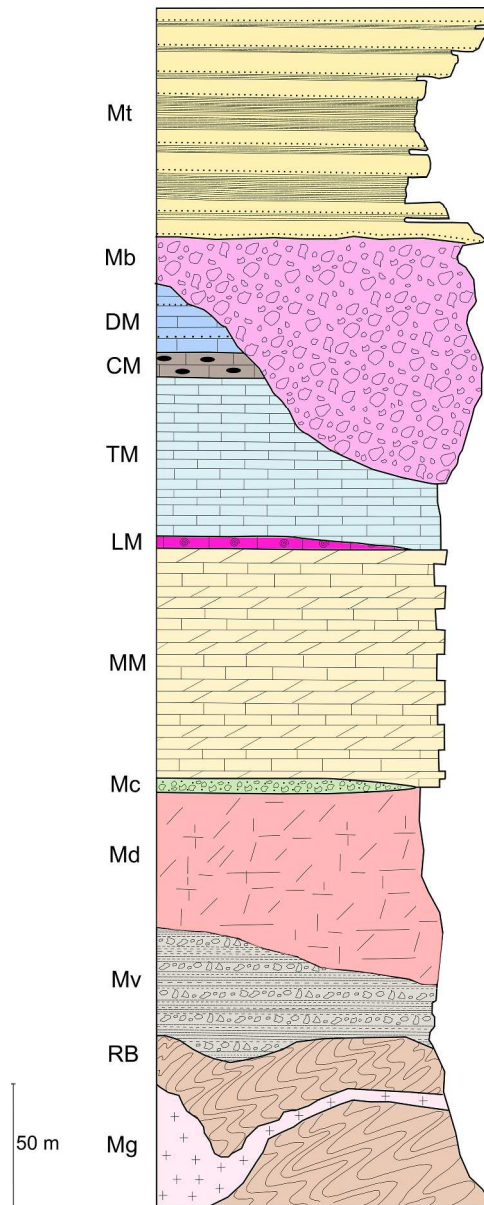


Figure 3. Reconstruction of the complete stratigraphic log of the Piedigriggio - Prato Unit by integration of stratigraphic data from the study and the neighbouring areas. RB: Roches Brunes Fm., Mg: Metagranites Fm., Mv: Metavolcanites and Metavolcanoclastites Fm., Md: Metadolomites Fm., Mc: Metaconglomerates Fm., MM: Metalimestones and Metadolomites Fm., LM: Lumachella Metalimestones Fm., TM: Thin-bedded Metalimestones Fm., CM: Cherty Metalimestones Fm., DM: Detritic Metalimestones Fm., Mb: Metabreccias Fm., Mt: Metaturbidites Fm.

198x494mm (300 x 300 DPI)

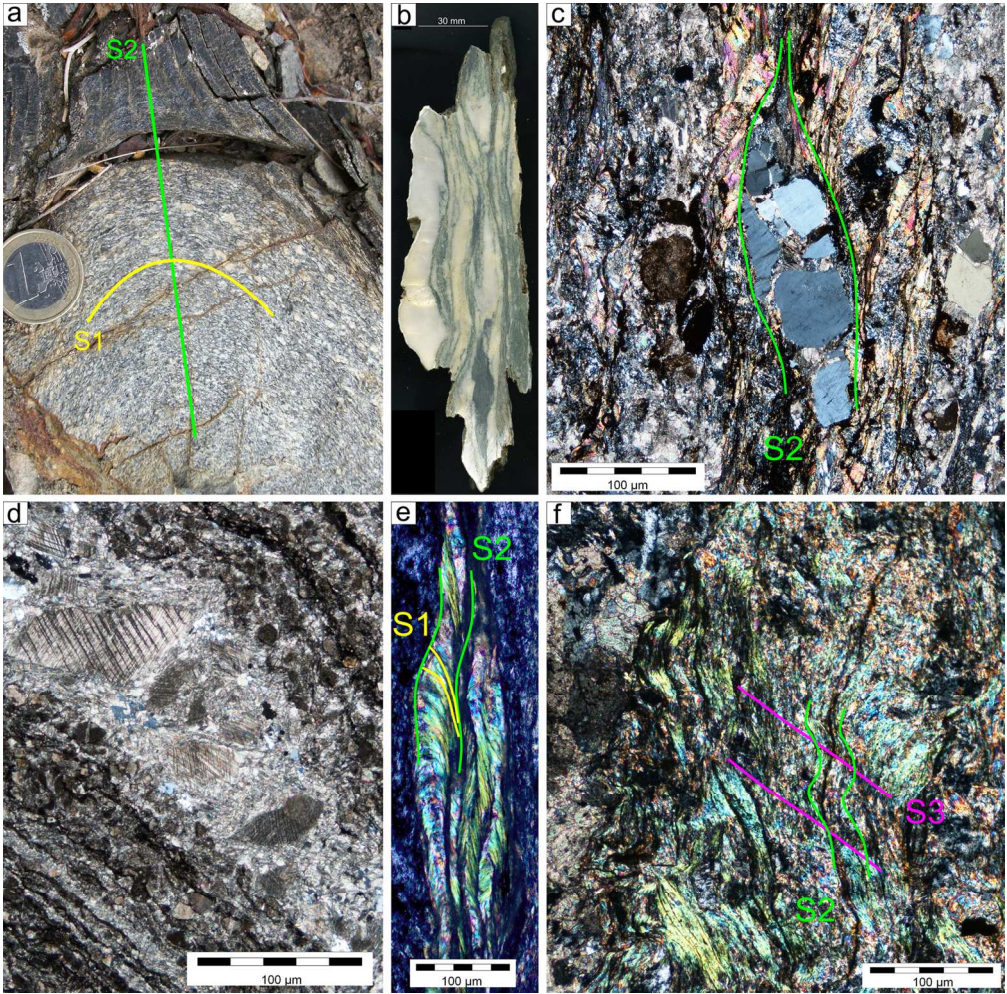


Figure 4. (A) F2 fold in Metaturbidites Fm. deforming lithological boundary, graded bedding and S1 foliation. (B) Metabreccias Fm. hand-sample showing high-ratio x:z flattened clasts. (C) Fractured porphyroclast wrapped by the S2 foliation in the Metabreccias Fm. (thin section, crossed nicols); (D) Crystals of calcite with type-2 twins in the Metabreccias Fm. (thin section, crossed nicols). (E) Relationship between S1 and S2 foliations in the matrix of the Metabreccias Fm. (thin section, crossed nicols). (F) S3 crenulation cleavage in the pelitic matrix of Metabreccias Fm. (I) F3 fold in Detritic Metalimestones Fm. (thin section, crossed nicols).

148x146mm (300 x 300 DPI)

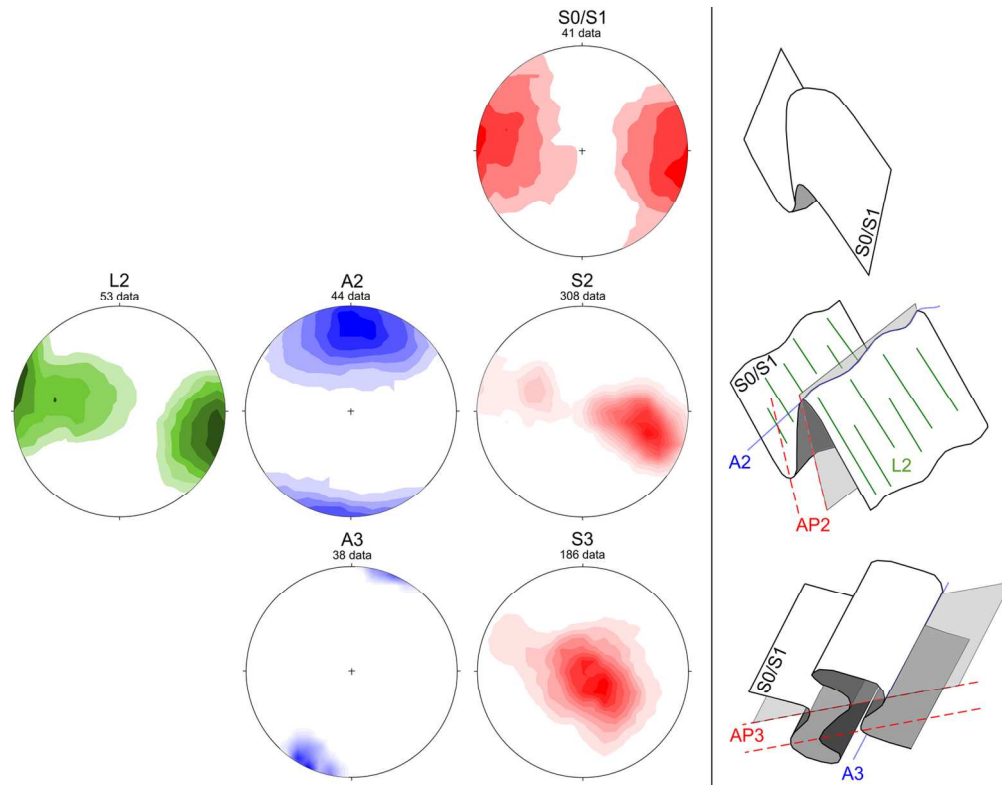


Figure 5. Stereographic plots of structural data collected in the study area (Schmidt net projection, lower hemisphere) and related schematic model of the folding. Density classes: 1% contour.

140x108mm (300 x 300 DPI)

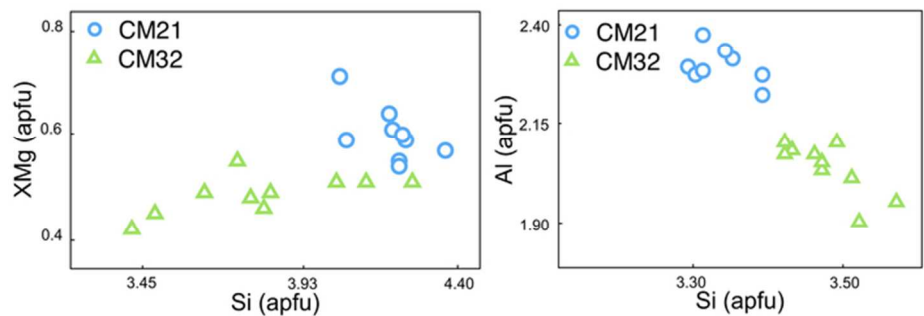


Figure 6. Si/XMg plot for chlorites (A) and Si/Al plot for phengites (B) of the studied samples.

64x23mm (300 x 300 DPI)

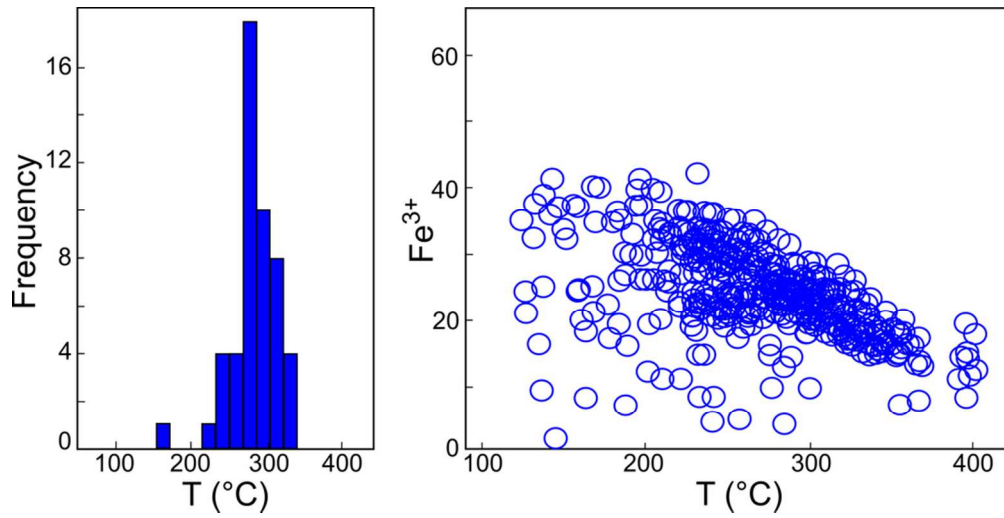


Figure 7. (A) Quantitative histogram of chlorites in equilibrium at different temperatures for sample CM21.
(B) Temperature vs. Fe³⁺ plot from the chlorites in sample CM32.

90x45mm (300 x 300 DPI)

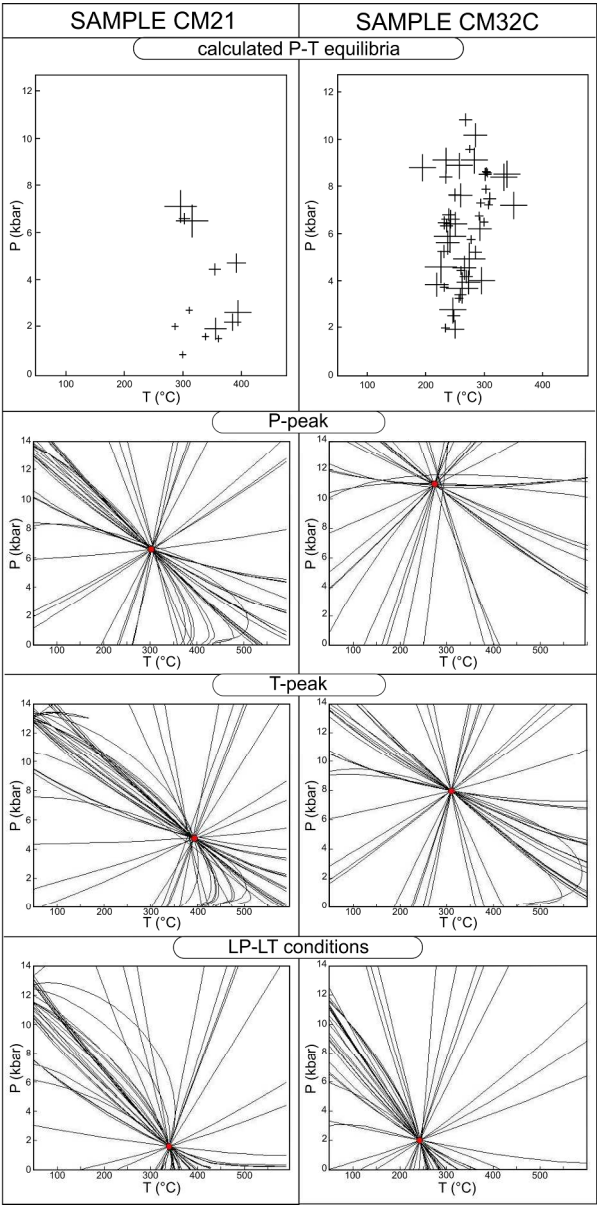


Figure 8. P-T equilibria conditions obtained with the application of the Chlorite-Phengite-Quartz-Water multiequilibrium approach on the CM21 and CM32C samples.

217x394mm (300 x 300 DPI)

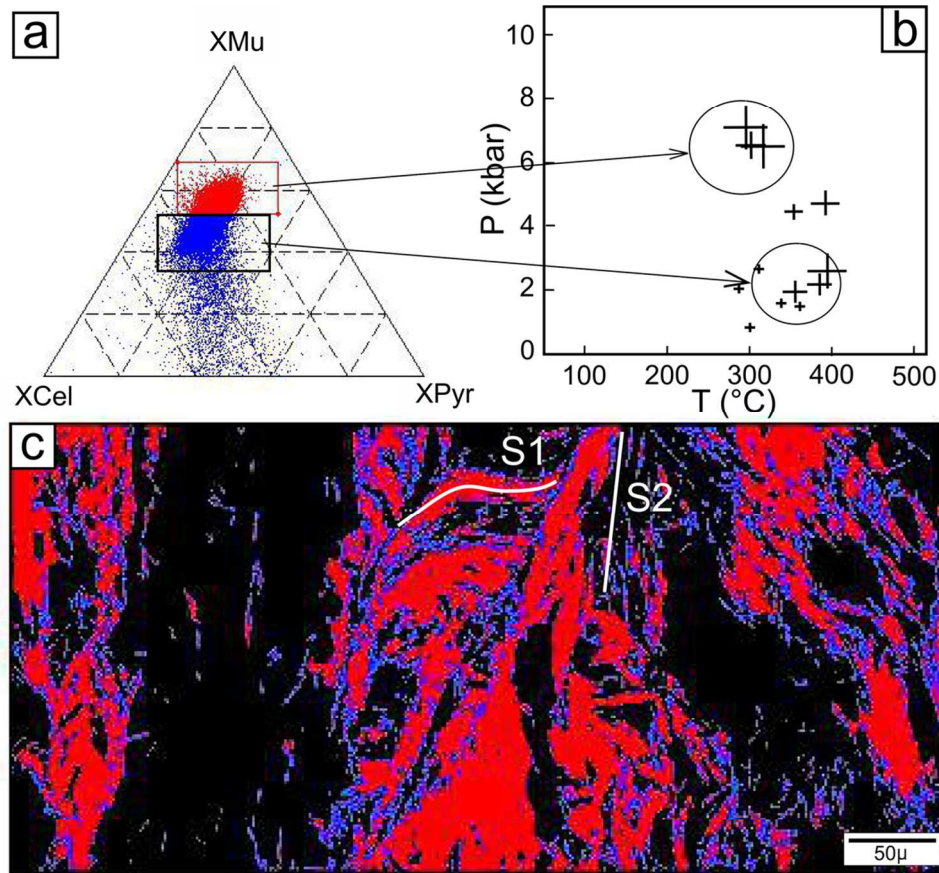


Figure 9. (A) Ternary diagram of phengite end-members for sample CM21 (XMU: muscovite, XCEL: celadonite, XPYR: pyrophyllite). Red points: phengites more enriched in the muscovitic end-member grown along the S1 foliation. Blue points: phengites enriched in the celadonitic end-member grown in the S2 foliation. (B) P-T path showing the equilibria conditions obtained for phengites plotted in (A). (C) Element map showing the phengites grew during the D1 phase (in red) and the D2 phase (in blue).

109x100mm (300 x 300 DPI)

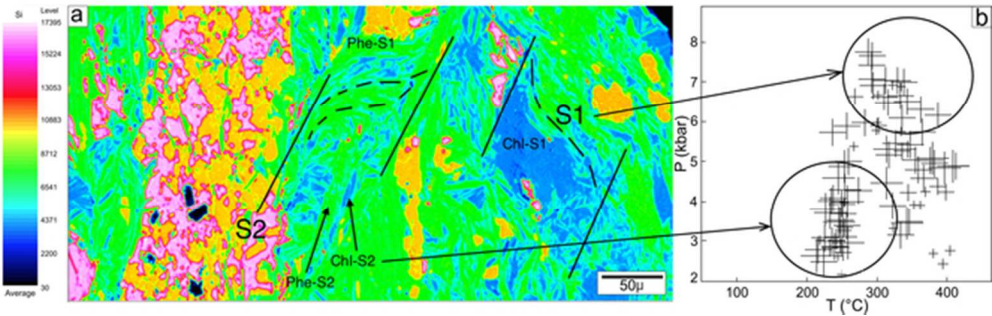


Figure 10. (A) Si-intensity map acquired with EPMA (sample CM21); five phases are identifiable: quartz (level 17395-11968), feldspar (level 11968-10000), phengite (level 10000-6500), chlorite (6500-3000). (B) P-T equilibria conditions of sample CM21. Arrows indicate the studied areas.

56x17mm (300 x 300 DPI)

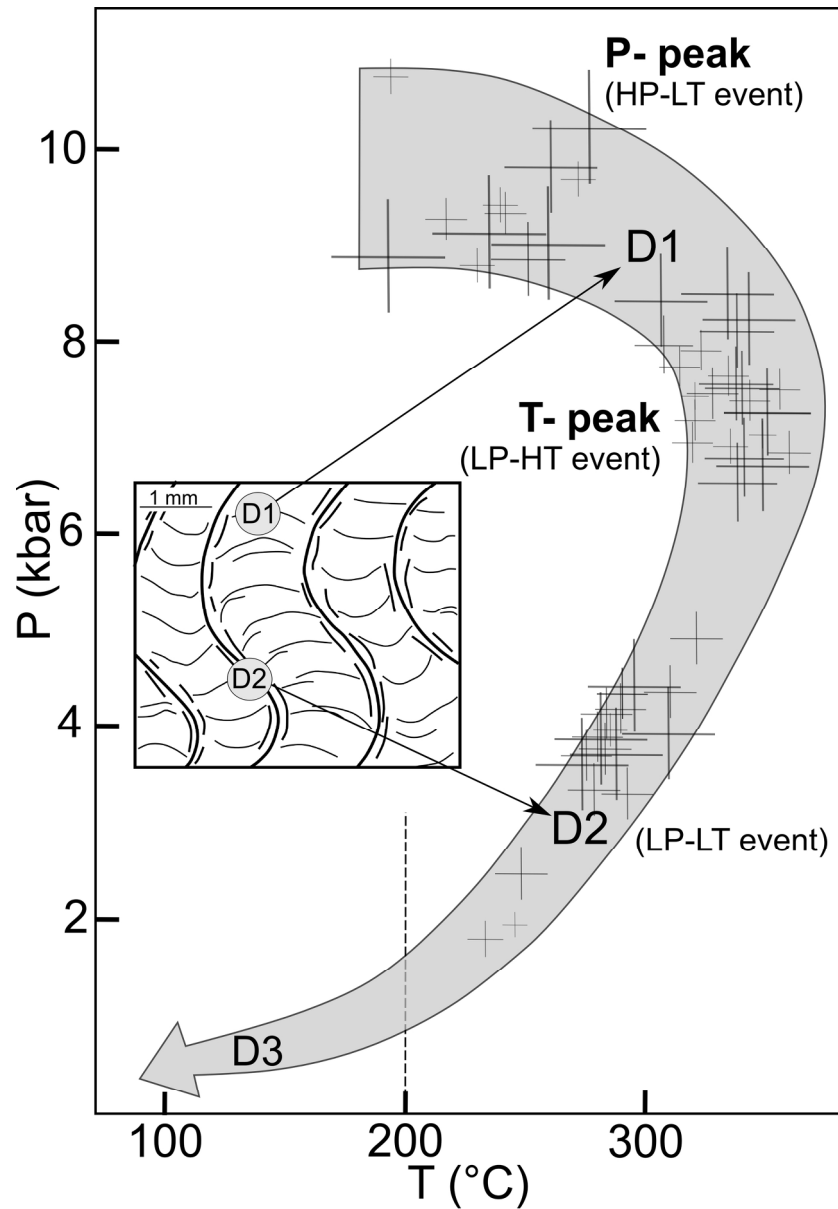


Figure 11. P-T-d path obtained for sample CM32C; the crosses indicate the P-T conditions calculated for the chlorite-phengite couples grew equilibria during the D1 and D2 phases. The dash lines at $T = 200^{\circ}\text{C}$ indicate the deformation temperature estimated for the D3 phase using calcite twins.

174x253mm (300 x 300 DPI)

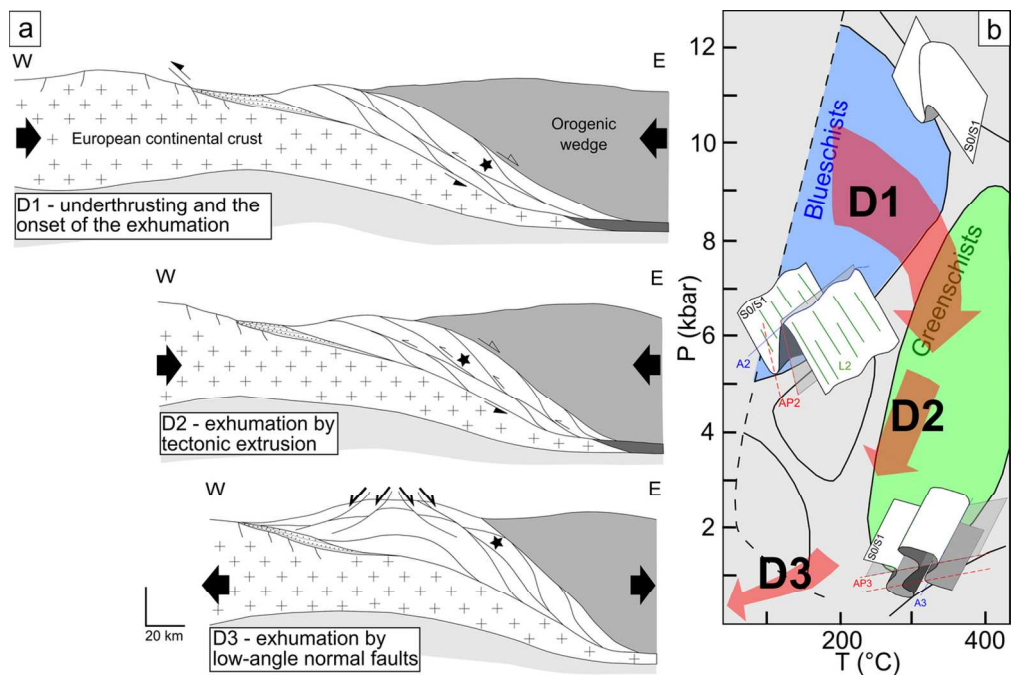


Figure 12. (A) Cartoon illustrating the tectono-metamorphic evolution of the Piedigreggio-Prato Unit (indicated with the star) during the Late Eocene-Oligocene time span. From the top of the bottom: underthrusting of the Piedigreggio-Prato Unit at depth of 30 km into the orogenic wedge during the D1 phase, followed by the onset of the exhumation; continuous exhumation during the D2 phase from ~ 30 km to ~10 km of depth; final stage of exhumation produced by extensional tectonics driven by low-angle normal faults during the D3 phase. (B) P-T-d path elaborated for the Piedigreggio-Prato Unit.

122x82mm (300 x 300 DPI)

Geothermometer	T max (°C)	
	SAMPLE CM21	SAMPLE CM32C
Bourdelle (2013)	271	228
Chatelineau (1988)	347	320
Chatelineau & Nieva (1985)	292	268
Hillier & Velde (1991)	315	279
Lanari (Fe ³⁺ =10%) (2014)	344	311

1
2
3
4
5
6
7
8
9
10
11
12
13
14
15
16
17
18
19
20
21
22
23
24
25
26
27
28
29
30
31
32
33
34
35
36
37
38
39
40
41
42
43
44
45
46
47
48
49
50
51
52
53
54
55
56
57
58
59
60

P (kbar)	SAMPLE CM21	SAMPLE CM32C
Max	11.91	12.66
Min	1.84	5.08

For Peer Review

Sample	CM21						CM32C					
Domain	S1(HP)		S1(HT)		S2		S1(HP)		S1(HT)		S2	
Analyse	chl31	phe18	chl18	phe13	chl12	phe5	chl7	phe7	chl9	phe2	chl10	phe1
Wt%												
SiO ₂	28.27	48.40	25.58	50.22	30.67	55.27	30.34	49.86	27.93	50.53	32.28	54.47
TiO ₂	0.02	0.11	0.03	0.12	0.03	0.21	0.03	0.05	0.03	0.17	0.03	0.10
Al ₂ O ₃	22.61	30.56	20.98	29.77	23.67	28.36	21.15	26.28	18.42	17.40	21.47	22.91
FeO	22.54	3.31	26.91	3.06	19.87	3.48	24.41	4.58	29.06	4.80	22.41	5.23
MnO	0.04	2.29	0.03	2.27	0.03	0.03	0.46	0.04	0.54	0.04	0.42	0.03
MgO	13.99	0.03	13.36	0.03	13.19	3.62	11.59	2.76	11.63	3.82	10.74	3.10
CaO	0.04	0.01	0.04	0.01	0.03	0.02	0.09	0.03	0.11	0.07	0.11	0.06
Na ₂ O	0.05	0.14	0.05	0.15	0.05	0.04	0.04	0.04	0.04	0.04	0.04	0.04
K ₂ O	0.68	8.98	0.06	9.01	1.12	8.29	0.88	8.36	0.24	8.30	1.39	7.70
tot.	88.24	93.83	87.04	94.64	88.66	99.32	88.99	92.00	88.00	85.17	88.89	92.64
Cations												
Si	3.10	3.48	2.91	3.56	3.29	3.69	3.28	3.64	3.13	3.96	3.44	3.85
Ti	-	0.01	-	0.01	-	0.01	-	-	-	0.01	-	0.01
Al	2.48	2.20	2.39	2.11	2.54	1.89	2.29	1.92	2.06	1.36	2.29	1.62
Fe ²⁺	2.47	0.24	3.06	0.22	2.13	0.23	2.64	0.33	3.25	0.38	2.39	0.37
Mn	-	0.16	-	0.16	-	-	0.05	-	0.06	-	0.04	-
Mg	1.54	-	1.52	-	1.41	0.24	1.25	0.20	1.30	0.30	1.15	0.22
Ca	-	-	-	-	-	-	0.01	-	0.01	0.01	0.01	-
Na	0.01	0.01	0.01	0.01	0.01	-	-	-	-	-	-	-
K	0.07	0.65	0.01	0.64	0.12	0.55	0.10	0.61	0.03	0.65	0.15	0.54
sum ox	14.00	11.00	14.00	11.00	14.00	11.00	14.00	11.00	14.00	11.00	14.00	11.00

- : below detection limits.